

Electronic Supplementary Information on

The influence of copper on the optical band gap of heterometallic iodido antimonates and bismuthates

Jakob Möbs,^a Jan-Niclas Luy,^b Alena Shlyaykher,^a Ralf Tonner^b and Johanna Heine^{a}*

^a Department of Chemistry and Material Sciences Center, Philipps-Universität Marburg, Hans-Meerwein-Straße, 35043 Marburg, Germany. E-mail: johanna.heine@chemie.uni-marburg.de.

^b Wilhelm-Ostwald-Institut für Physikalische und Theoretische Chemie, Universität Leipzig, Linnéstraße 2, 04103 Leipzig, Germany.

Table of contents

Additional synthetic procedures	2
Additional crystallographic details	3
Additional crystal structures that are not discussed in the main article	24
Thermal analysis	33
Optical properties.....	40
Powder diffraction.....	47
IR spectroscopy	55
Theoretical investigations	56
References.....	64

Additional synthetic procedures

For better comparability we reproduced $[\text{NBu}_4][\text{Bi}_2\text{I}_{10}(\text{CuP}(\text{OPh})_3)_2]$ (**A**) and $[\text{NBu}_4][\text{Bi}_2\text{I}_{10}(\text{CuPPh}_3)_2]$ (**B**) by *Pike* and co-workers.¹ We were able to simplify the syntheses slightly and also to obtain crystals of solvent free $[\text{NBu}_4][\text{Bi}_2\text{I}_{10}(\text{CuPPh}_3)_2]$ suitable for x-ray diffraction, while the group of *Pike* only published the crystal structure of $[\text{NBu}_4][\text{Bi}_2\text{I}_{10}(\text{CuPPh}_3)_2] \cdot \text{MeCN}$.

$[\text{NBu}_4][\text{Bi}_2\text{I}_{10}(\text{CuP}(\text{OPh})_3)_2]$ (A): A total of 59 mg of BiI_3 (0.1 mmol), 19 mg of CuI (0.1 mmol), 26 μL of $\text{P}(\text{OPh})_3$ (0.1 mmol) and 37 mg of NBu_4I (0.1 mmol) were suspended in 10 mL of isopropanol, heated to 90 °C for 1 h under reflux cooling and then stirred at room temperature for two days. The orange powder was collected, washed twice with 3 mL of cold ethanol and once with 3 mL of *n*-pentane yielding 133 mg of **A** (91 %). CHN (calculated for $\text{C}_{68}\text{H}_{102}\text{Bi}_2\text{Cu}_2\text{I}_{10}\text{N}_2\text{O}_6\text{P}_2$): C 27.23 (27.97), H 3.54 (3.52), N 1.03 (0.96). The slightly too small experimental value for carbon can be assigned to negligibly small amounts of unreacted CuI .

$[\text{NBu}_4][\text{Bi}_2\text{I}_{10}(\text{CuPPh}_3)_2]$ (B): A total of 59 mg of BiI_3 (0.1 mmol), 19 mg of CuI (0.1 mmol), 26 mg of PPh_3 (0.1 mmol) and 37 mg of NBu_4I (0.1 mmol) were suspended in 10 mL of ethanol and heated to 90 °C for 1 h under reflux cooling until a bright red powder had formed. After cooling to room temperature, the powder was collected, washed twice with 3 mL of cold ethanol and once with 3 mL of *n*-pentane yielding 125 mg of **B** (89 %). CHN (calculated for $\text{C}_{68}\text{H}_{102}\text{Bi}_2\text{Cu}_2\text{I}_{10}\text{N}_2\text{P}_2$): C 28.81 (28.93), H 3.69 (3.64), N 1.03 (0.99).

Single crystals were grown from a similarly prepared solution of the starting materials in dme over the course of three days at room temperature.

Additional crystallographic details

Single crystal X-ray determination was performed on a Bruker Quest D8 diffractometer with microfocus MoK α radiation ($\lambda = 0.71073$) and a Photon 100 (CMOS) detector, a STOE STADIVARI diffractometer with microfocus CuK α radiation and a Pilatus 300K (Dectris) detector or a STOE IPDS-2/2T diffractometer equipped with an imaging plate detector system using parallel beam MoK α radiation with graphite monochromatization.

Table S1: Crystallographic data for **1a**, measured on a Bruker D8 Quest at 100 K, CCDC 2102781.

	1a
Empirical formula	C ₆₃ H ₆₄ Cu ₂ I ₆ P ₃ Sb
Formula weight	1924.28
Temperature/K	100.0
Crystal system	trigonal
Space group	<i>R</i> -3
<i>a</i> /Å	15.8066(5)
<i>b</i> /Å	15.8066(5)
<i>c</i> /Å	22.7061(6)
α /°	90
β /°	90
γ /°	120
Volume/Å ³	4913.0(3)
<i>Z</i>	3
ρ_{calc} /g/cm ³	1.951
μ /mm ⁻¹	3.991
Absorption correction (<i>T</i> _{min} / <i>T</i> _{max})	multi-scan (0.1775/0.3312)
<i>F</i> (000)	2742.0
Crystal size/mm ³	0.1 × 0.089 × 0.065
Radiation	MoK α ($\lambda = 0.71073$)
2 θ range for data collection/°	4.662 to 50.88
Index ranges	-19 ≤ <i>h</i> ≤ 19, -19 ≤ <i>k</i> ≤ 19, -27 ≤ <i>l</i> ≤ 27
Reflections collected	33984
Independent reflections	2024 [<i>R</i> _{int} = 0.0468, <i>R</i> _{sigma} = 0.0168]
Data/restraints/parameters	2024/285/237
Goodness-of-fit on <i>F</i> ²	1.182
Final <i>R</i> indexes [<i>I</i> ≥ 2 σ (<i>I</i>)]	<i>R</i> ₁ = 0.0364, <i>wR</i> ₂ = 0.0647
Final <i>R</i> indexes [all data]	<i>R</i> ₁ = 0.0510, <i>wR</i> ₂ = 0.0695
Largest diff. peak/hole / e Å ⁻³	0.85/-0.84

Details of crystal structure measurement and refinement: AFIX 66 constraints had to be used on all phenyl rings to ensure a stable refinement. The *o*-tolyl phosphonium ion is disordered over six

positions which are linked by the $\bar{3}$ symmetry and have occupancies of $\frac{1}{6}$ each. Various SADI, ISOR, RIGU, and FLAT restraints had to be used here. All non-hydrogen atoms were refined anisotropically. Hydrogen atoms were assigned to idealized geometric positions and included in structure factors calculations.

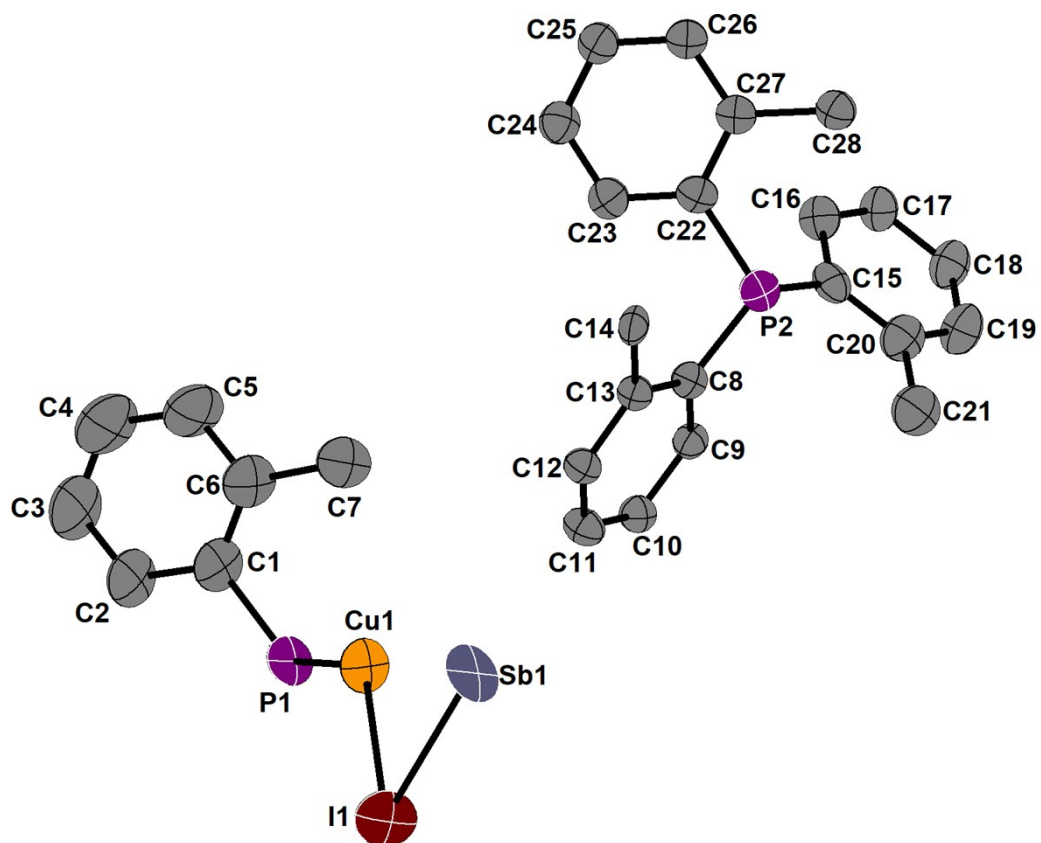


Figure S1: Asymmetric unit of **1a**. Hydrogen atoms are omitted for clarity.

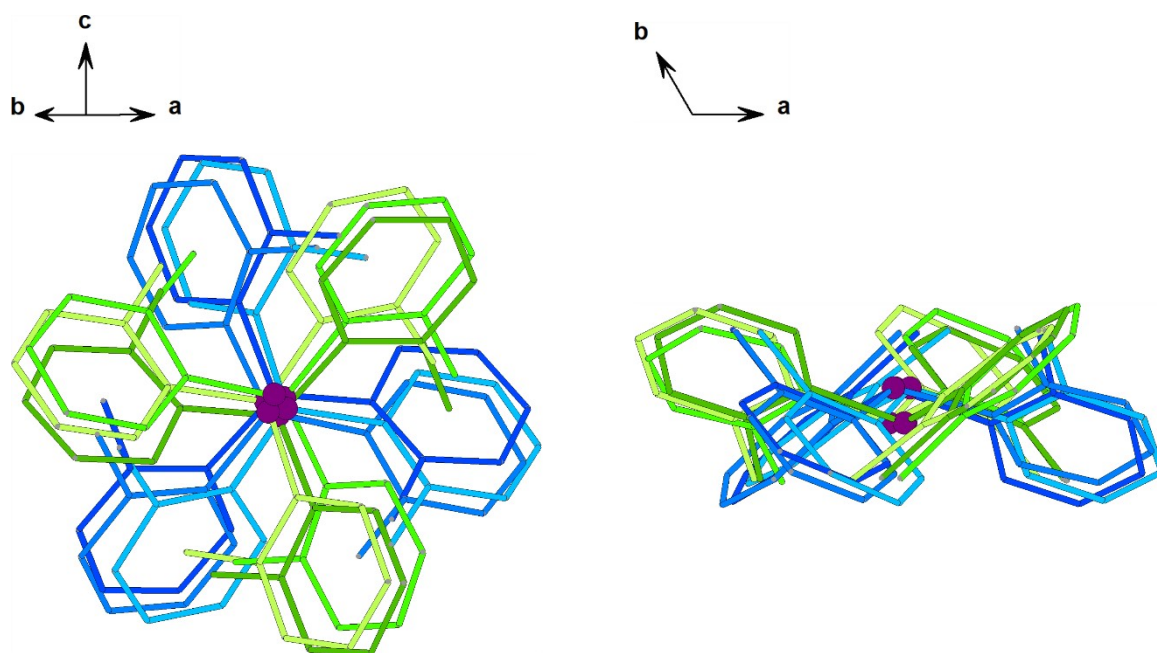


Figure S2: Disorder of the $[\text{HP}(o\text{-tol})_3]^+$ -cation of **1a**. The parts that are oriented in the same direction with regard to the $\bar{1}$ symmetry are shown in the same hue. *o*-tol-groups are shown only as frames, phosphor positions are shown as balls with a diameter of 0.2 Å. Hydrogen atoms are omitted for clarity.

All atom positions have an occupancy of $\frac{1}{6}$.

Table S2: Crystallographic data for **2a**, measured on a Bruker D8 Quest at 100 K, CCDC 2102778.

	2a
Empirical formula	C ₁₄₄ H ₁₅₅ Cu ₄ I ₂₁ N ₉ P ₆ Sb ₅
Formula weight	5725.45
Temperature/K	100
Crystal system	hexagonal
Space group	<i>P</i> 6 ₃
a/Å	14.9870(10)
b/Å	14.9870(10)
c/Å	44.289(2)
α/°	90
β/°	90
γ/°	120
Volume/Å ³	8615.0(12)
Z	2
ρ _{calc} /g/cm ³	2.207
μ/mm ⁻¹	5.120
Absorption correction (T _{min} /T _{max})	multi-scan (0.6286/0.7452)
F(000)	5312.0
Crystal size/mm ³	0.161 × 0.141 × 0.022
Radiation	MoKα (λ = 0.71073)
2θ range for data collection/°	4.836 to 50.722
Index ranges	-18 ≤ h ≤ 18, -18 ≤ k ≤ 18, -53 ≤ l ≤ 53
Reflections collected	123138
Independent reflections	10521 [R _{int} = 0.2247, R _{sigma} = 0.1101]
Data/restraints/parameters	10521/327/540
Goodness-of-fit on F ²	1.056
Final R indexes [I ≥ 2σ (I)]	R ₁ = 0.0681, wR ₂ = 0.1145
Final R indexes [all data]	R ₁ = 0.1121, wR ₂ = 0.1276
Largest diff. peak/hole / e Å ⁻³	4.69/-2.39
Flack parameter	0.36(7)

Details of crystal structure measurement and refinement: The crystals of **2a** were systematically twinned after (-1, 0, 0, 0, -1, 0, 0, 0, -1) and of low quality. This resulted in quite high R-values, especially an R_{int} of 22.47 %. An AFIX 66 and EADP constraint had to be used on one of the phenyl groups (C15 – C20) in addition to ISOR restraints on all carbon and nitrogen atoms as well as on P1, P3 and Cu4 to ensure a stable refinement. All non-hydrogen atoms were refined anisotropically. Hydrogen atoms were assigned to idealized geometric positions and included in structure factors calculations. The phosphorous-bonded hydrogen atoms of the protonated phosphines needed to be fixed in place using DFIX restraints.

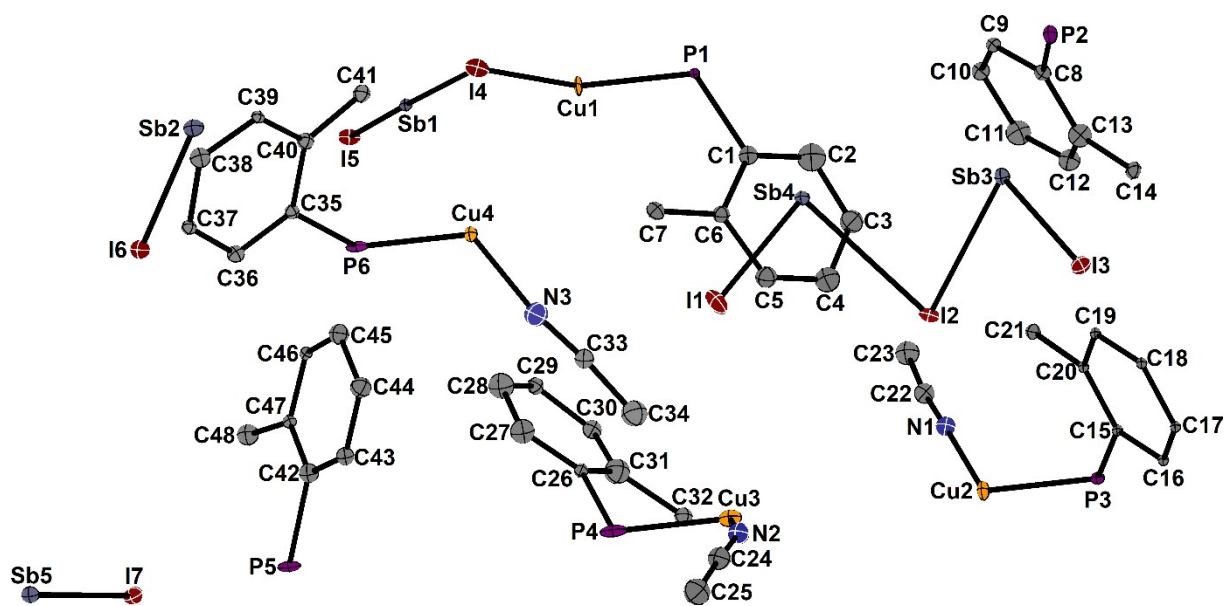


Figure S3: Asymmetric unit of **2a**, ellipsoids at 50 % probability. Hydrogen atoms are omitted for clarity.

Table S3: Crystallographic data for **2b**, measured on a Bruker D8 Quest at 100 K, CCDC 2102780.

	2b
Empirical formula	C ₁₄₄ H ₁₅₅ Bi ₅ Cu ₄ I ₂₁ N ₉ P ₆
Formula weight	6161.60
Temperature/K	100.0
Crystal system	hexagonal
Space group	<i>P</i> 6 ₃
a/Å	14.9871(5)
b/Å	14.9871(5)
c/Å	44.5600(17)
α/°	90
β/°	90
γ/°	120
Volume/Å ³	8667.8(7)
Z	2
ρ _{calc} /g/cm ³	2.361
μ/mm ⁻¹	9.378
Absorption correction (T _{min} /T _{max})	multi-scan (0.0011/ 0.0097)
F(000)	5632.0
Crystal size/mm ³	0.228 × 0.128 × 0.041
Radiation	MoKα (λ = 0.71073)
2θ range for data collection/°	4.818 to 50.694
Index ranges	-18 ≤ h ≤ 17, -17 ≤ k ≤ 18, -53 ≤ l ≤ 53
Reflections collected	71055
Independent reflections	10523 [R _{int} = 0.0992, R _{sigma} = 0.0837]
Data/restraints/parameters	10523/219/578
Goodness-of-fit on F ²	1.032
Final R indexes [I ≥ 2σ (I)]	R ₁ = 0.0456, wR ₂ = 0.0703
Final R indexes [all data]	R ₁ = 0.0750, wR ₂ = 0.0766
Largest diff. peak/hole / e Å ⁻³	3.09/-0.98
Flack parameter	0.214(7)

Details of crystal structure measurement and refinement: As with the isostructural **2a** the crystals of **2b** were systematically twinned after (-1, 0, 0, 0, -1, 0, 0, 0, -1) but of slightly better quality. Still residue electron density is found along the six-fold axis that we attribute to the poor data quality and additional twin domains. ISOR restraints had to be used on most of the carbon atoms (C1 – C8, C12 – C17, C19 – C26, C28 – C40) and on N3 to ensure a stable refinement. All non-hydrogen atoms were refined anisotropically. Hydrogen atoms were assigned to idealized geometric positions and included in structure factors calculations. The phosphorous-bonded hydrogen atoms of the protonated phosphines needed to be fixed in place using DFIX restraints.

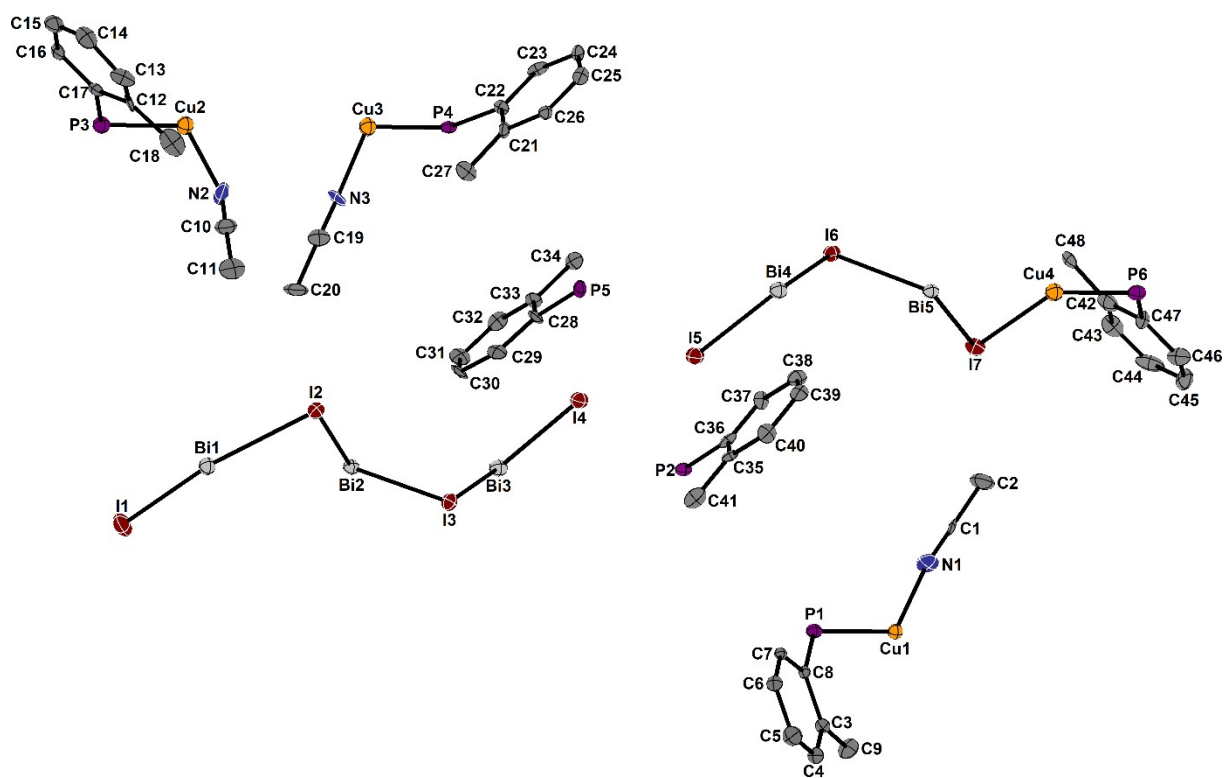


Figure S4: Asymmetric unit of **2b**, ellipsoids at 50 % probability. Hydrogen atoms are omitted for clarity.

Table S4: Crystallographic data for **3a**, measured on a Stoe StadiVari at 100 K, CCDC 2102782.

	3a
Empirical formula	C _{113.41} H _{128.11} Cu ₄ I ₂₂ N _{14.01} P ₄ Sb ₆
Formula weight	5597.64
Temperature/K	100.0
Crystal system	trigonal
Space group	<i>P</i> -3
a/Å	14.7250(2)
b/Å	14.7250(2)
c/Å	22.9033(6)
α/°	90
β/°	90
γ/°	120
Volume/Å ³	4300.70(16)
Z	1
ρ _{calc} /g/cm ³	2.161
μ/mm ⁻¹	39.543
Absorption correction (T _{min} /T _{max})	numerical, multi-scan (0.0000/ 0.0000)
F(000)	2560.0
Crystal size/mm ³	0.19891 × 0.15485 × 0.12238
Radiation	CuKα (λ = 1.54178)
2θ range for data collection/°	6.932 to 151.448
Index ranges	-11 ≤ h ≤ 18, -18 ≤ k ≤ 13, -28 ≤ l ≤ 23
Reflections collected	32766
Independent reflections	5930 [R _{int} = 0.0328, R _{sigma} = 0.0286]
Data/restraints/parameters	5930/9/276
Goodness-of-fit on F ²	0.994
Final R indexes [I ≥ 2σ (I)]	R ₁ = 0.0695, wR ₂ = 0.1732
Final R indexes [all data]	R ₁ = 0.0814, wR ₂ = 0.1786
Largest diff. peak/hole / e Å ⁻³	2.16/-0.55

Details of crystal structure measurement and refinement: All non-hydrogen atoms were refined anisotropically with the exception of the carbon and nitrogen atoms in the disordered and only partially occupied acetonitrile moieties. These molecules were modelled using the FragmentDB / DSR² and DFIX restraints needed to be applied to give a meaningful model. The occupancies of N1_4, C1_4 and C2_4 were refined freely to 12% using one free variable, while the occupancies of C1_3 / C2_3 and C3 / C4 were refined to 22 % and 34 %, respectively, using one free variable for each pair. Hydrogen atoms were assigned to idealized geometric positions and included in structure factors calculations.

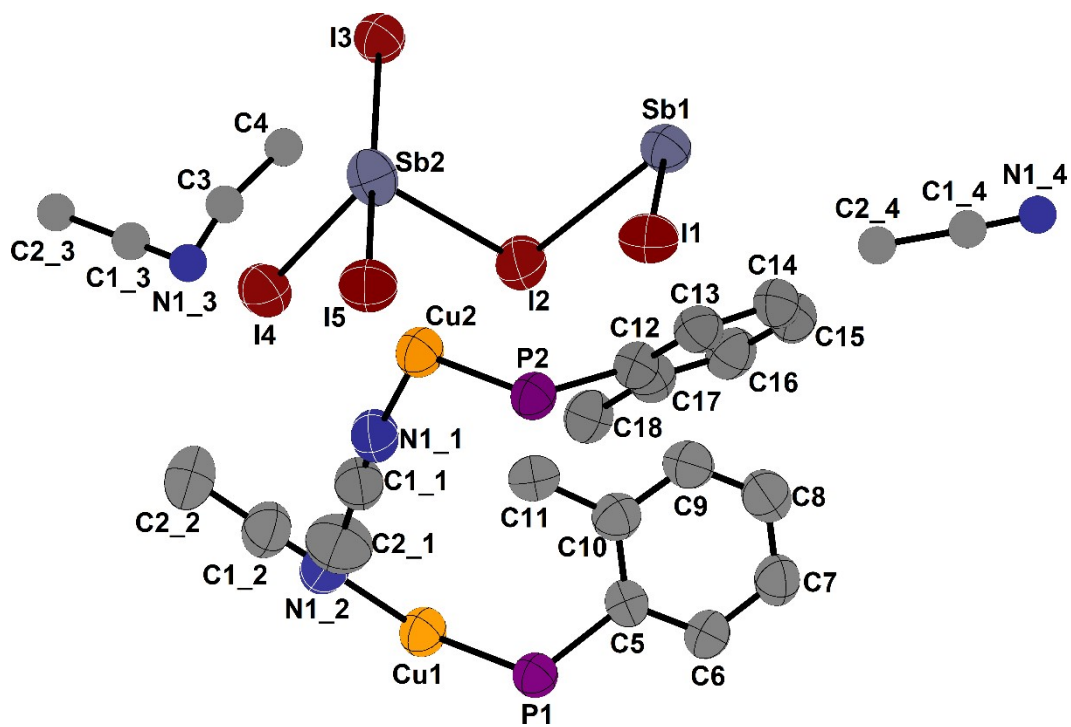


Figure S5: Asymmetric unit of **3a**, ellipsoids at 50 % probability, isotropically refined atoms are shown as spheres with a diameter of 0.3 Å. Hydrogen atoms are omitted for clarity.

Table S5: Crystallographic data for **3b**, measured on a Stoe IPDS2 at 100 K, CCDC 2102784.

3b	
Empirical formula	C ₁₀₈ H ₁₂₀ Bi ₆ Cu ₄ I ₂₂ N ₁₂ P ₄
Formula weight	6009.87
Temperature/K	100
Crystal system	trigonal
Space group	<i>P</i> -3
<i>a</i> /Å	14.6948(7)
<i>b</i> /Å	14.6948(7)
<i>c</i> /Å	23.2365(13)
α /°	90
β /°	90
γ /°	120
Volume/Å ³	4345.4(5)
<i>Z</i>	1
ρ_{calc} /cm ³	2.297
μ /mm ⁻¹	10.512
Absorption correction (<i>T</i> _{min} / <i>T</i> _{max})	numerical (0.1476/ 0.3830)
<i>F</i> (000)	2760.0
Crystal size/mm ³	0.25687 × 0.17193 × 0.10073
Radiation	MoK α (λ = 0.71073)
2 θ range for data collection/°	3.2 to 53.71
Index ranges	-18 ≤ <i>h</i> ≤ 18, -18 ≤ <i>k</i> ≤ 18, -29 ≤ <i>l</i> ≤ 29
Reflections collected	28417
Independent reflections	6226 [<i>R</i> _{int} = 0.0684, <i>R</i> _{sigma} = 0.0591]
Data/restraints/parameters	6226/0/248
Goodness-of-fit on <i>F</i> ²	0.947
Final <i>R</i> indexes [<i>I</i> ≥ 2 σ (<i>I</i>)]	<i>R</i> ₁ = 0.0321, <i>wR</i> ₂ = 0.0732
Final <i>R</i> indexes [all data]	<i>R</i> ₁ = 0.0553, <i>wR</i> ₂ = 0.0768
Largest diff. peak/hole / e Å ⁻³	1.53/-1.86

Details of crystal structure measurement and refinement: The crystal was merohedrally twinned after (0, -1, 0, -1, 0, 0, 0, 0, -1). Strongly disordered and only partially occupied MeCN-molecules were found, that could not be refined sufficiently. To account for this a solvent mask with 37 electrons in two voids was applied. This fits overall 1.75 molecules of MeCN. All non-hydrogen atoms were refined anisotropically. Hydrogen atoms were assigned to idealized geometric positions and included in structure factors calculations.

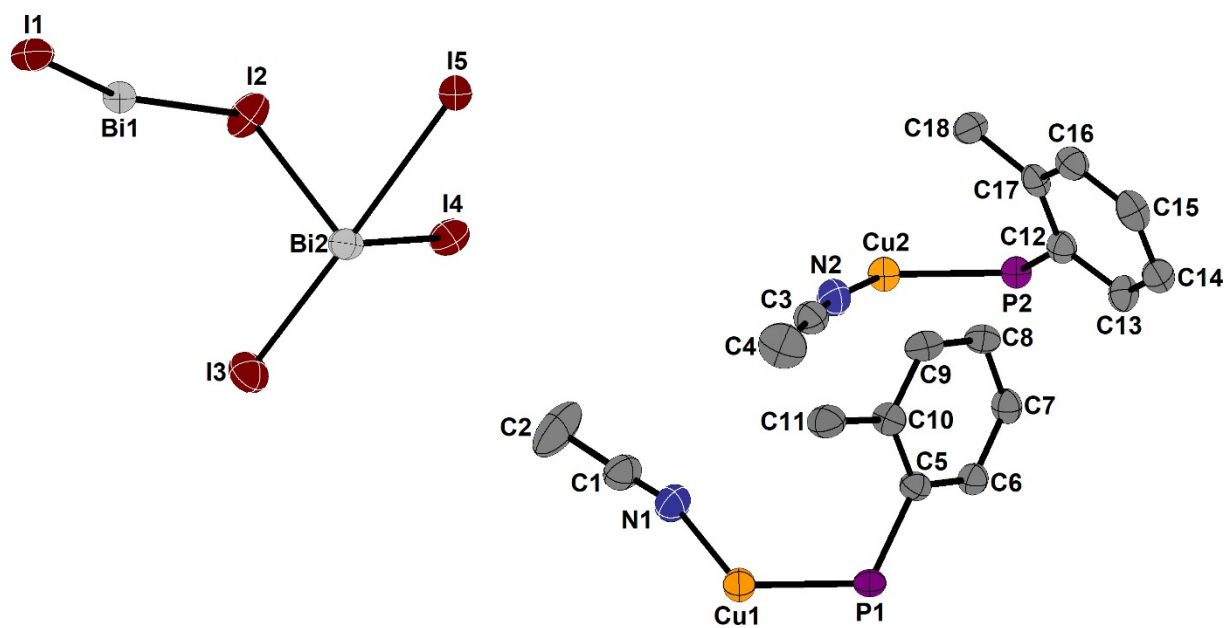


Figure S6: Asymmetric unit of **3b**, ellipsoids at 50 % probability. Hydrogen atoms are omitted for clarity.

Table S6: Crystallographic data for **4**, measured on a Stoe StadiVari at 100 K, CCDC 2102783.

	4
Empirical formula	C ₄₅ H ₄₈ BiCu ₂ I ₅ OP ₂
Formula weight	1637.33
Temperature/K	100
Crystal system	orthorhombic
Space group	<i>Pna2</i> ₁
a/Å	17.9943(12)
b/Å	17.7272(13)
c/Å	15.8671(9)
α/°	90
β/°	90
γ/°	90
Volume/Å ³	5061.4(6)
Z	4
ρ _{calc} /g/cm ³	2.149
μ/mm ⁻¹	32.472
Absorption correction (T _{min} /T _{max})	numerical, multi-scan (0.0007/ 0.0087)
F(000)	3048.0
Crystal size/mm ³	0.15798 × 0.05098 × 0.0504
Radiation	Cu Kα (λ = 1.54178)
2θ range for data collection/°	7 to 151.432
Index ranges	-21 ≤ h ≤ 22, -22 ≤ k ≤ 21, -19 ≤ l ≤ 12
Reflections collected	126688
Independent reflections	8754 [R _{int} = 0.0486, R _{sigma} = 0.0295]
Data/restraints/parameters	8754/1/514
Goodness-of-fit on F ²	0.968
Final R indexes [I ≥ 2σ (I)]	R ₁ = 0.0241, wR ₂ = 0.0523
Final R indexes [all data]	R ₁ = 0.0283, wR ₂ = 0.0530
Largest diff. peak/hole / e Å ⁻³	1.20/-0.75
Flack parameter	0.068(8)

Details of crystal structure measurement and refinement: The crystal was merohedrally twinned after (-1, 0, 0, 0, -1, 0, 0, 0, -1). All non-hydrogen atoms were refined anisotropically. Hydrogen atoms were assigned to idealized geometric positions and included in structure factors calculations.

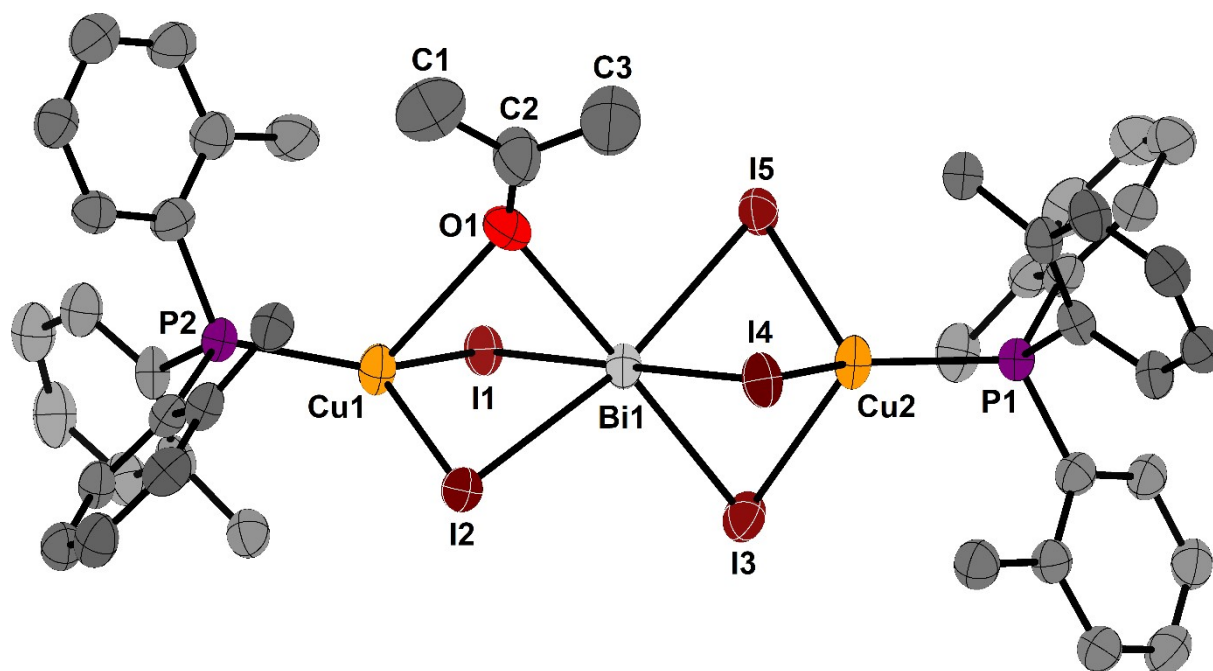


Figure S7: Asymmetric unit of **4**, ellipsoids at 50 % probability. Hydrogen atoms and atom labels of the tolyl groups are omitted for clarity.

Table S7: Crystallographic data for **5a**, measured on a Stoe StadiVari at 100 K, CCDC 2102785.

	5a
Empirical formula	C ₈₄ H ₈₄ Cu ₂ I ₁₂ P ₄ Sb ₂
Formula weight	3110.77
Temperature/K	100
Crystal system	triclinic
Space group	<i>P</i> -1
<i>a</i> /Å	14.1928(2)
<i>b</i> /Å	14.5293(2)
<i>c</i> /Å	14.6615(4)
α /°	117.9820(10)
β /°	104.6040(10)
γ /°	105.1260(10)
Volume/Å ³	2315.30(8)
<i>Z</i>	1
ρ_{calc} /cm ³	2.231
μ /mm ⁻¹	37.467
Absorption correction (<i>T</i> _{min} / <i>T</i> _{max})	numerical, multi-scan (0.0000/ 0.0004)
<i>F</i> (000)	1444.0
Crystal size/mm ³	0.126 × 0.111 × 0.105
Radiation	CuK α (λ = 1.54178)
2 θ range for data collection/°	7.066 to 135
Index ranges	-17 ≤ <i>h</i> ≤ 17, -16 ≤ <i>k</i> ≤ 17, -17 ≤ <i>l</i> ≤ 17
Reflections collected	59560
Independent reflections	8276 [<i>R</i> _{int} = 0.0418, <i>R</i> _{sigma} = 0.0341]
Data/restraints/parameters	8276/0/475
Goodness-of-fit on <i>F</i> ²	0.950
Final <i>R</i> indexes [<i>I</i> ≥ 2 σ (<i>I</i>)]	<i>R</i> ₁ = 0.0357, <i>wR</i> ₂ = 0.0864
Final <i>R</i> indexes [all data]	<i>R</i> ₁ = 0.0455, <i>wR</i> ₂ = 0.0889
Largest diff. peak/hole / e Å ⁻³	1.74/-0.62

Details of crystal structure measurement and refinement: All non-hydrogen atoms were refined anisotropically. Hydrogen atoms were assigned to idealized geometric positions and included in structure factors calculations.

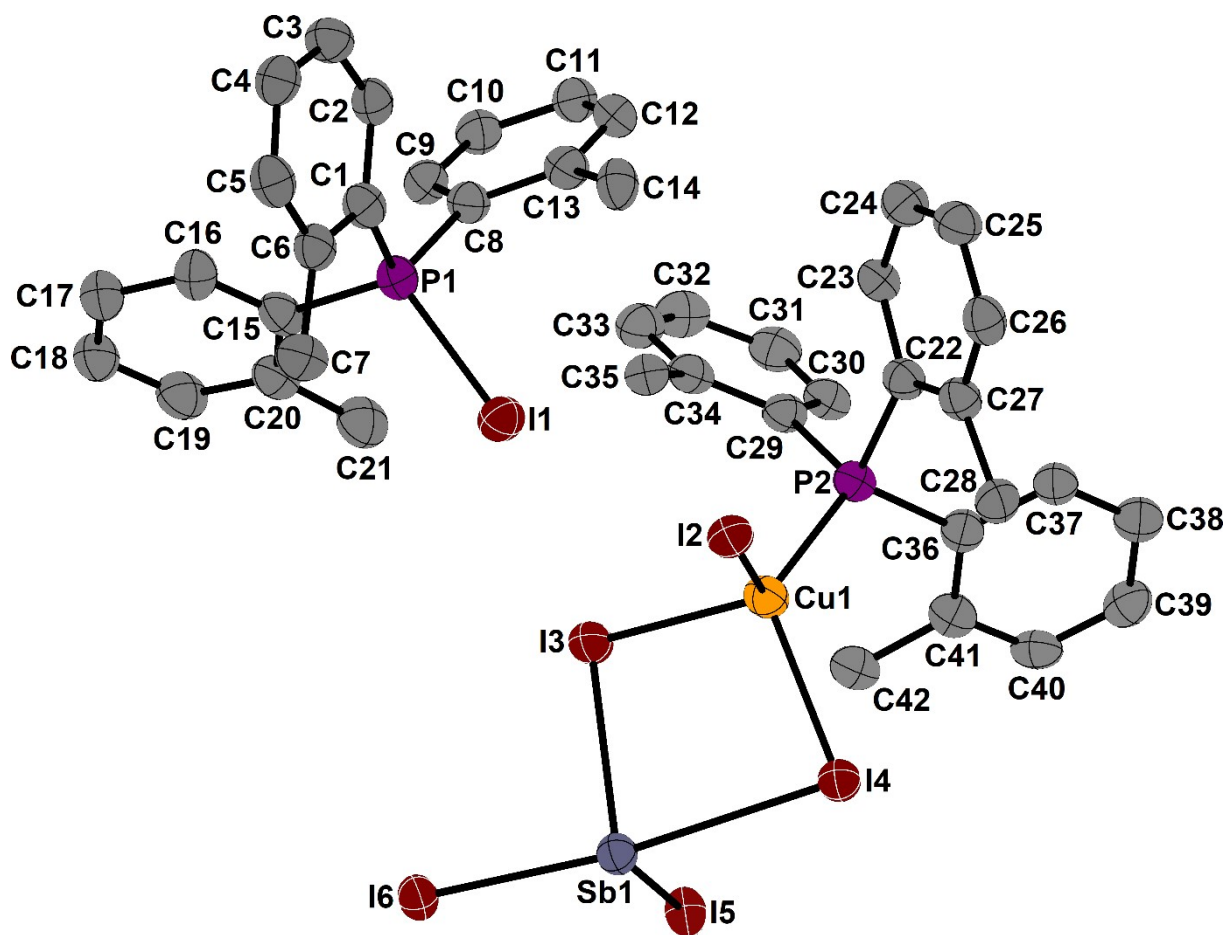


Figure S8: Asymmetric unit of 5a, ellipsoids at 50 % probability. Hydrogen atoms are omitted for clarity.

Table S8: Crystallographic data for **5b**, measured on a Stoe StadiVari at 100 K, CCDC 2102774.

	5b
Empirical formula	C ₈₄ H ₈₄ Bi ₂ Cu ₂ I ₁₂ P ₄
Formula weight	3285.23
Temperature/K	100
Crystal system	triclinic
Space group	<i>P</i> -1
<i>a</i> /Å	14.2398(3)
<i>b</i> /Å	14.5995(3)
<i>c</i> /Å	14.7020(3)
α /°	105.454(2)
β /°	117.2590(10)
γ /°	105.296(2)
Volume/Å ³	2338.21(9)
<i>Z</i>	1
ρ_{calc} /cm ³	2.333
μ /mm ⁻¹	39.820
Absorption correction (<i>T</i> _{min} / <i>T</i> _{max})	multi-scan (0.0021/ 0.0175)
<i>F</i> (000)	1508.0
Crystal size/mm ³	0.106 × 0.065 × 0.047
Radiation	CuK α (λ = 1.54178)
2 θ range for data collection/°	7.036 to 140.204
Index ranges	-17 ≤ <i>h</i> ≤ 17, -16 ≤ <i>k</i> ≤ 17, -17 ≤ <i>l</i> ≤ 11
Reflections collected	59581
Independent reflections	8744 [<i>R</i> _{int} = 0.0671, <i>R</i> _{sigma} = 0.0479]
Data/restraints/parameters	8744/0/475
Goodness-of-fit on <i>F</i> ²	0.950
Final <i>R</i> indexes [<i>I</i> ≥ 2 σ (<i>I</i>)]	<i>R</i> ₁ = 0.0417, <i>wR</i> ₂ = 0.1002
Final <i>R</i> indexes [all data]	<i>R</i> ₁ = 0.0613, <i>wR</i> ₂ = 0.1069
Largest diff. peak/hole / e Å ⁻³	1.85/-2.40

Details of crystal structure measurement and refinement: There is still some negative electron density to be found around I1 and when refined freely the occupancy will drop to only 87 %. However, we believe that this is only a feature of that individual crystal and that a full occupation of this position describes our compound best. The CHN results of the bulk material match nicely and we do not encounter the problem with the analogous antimony compound. Therefore we fixed the occupancy of I1 to 100 %. The missing charge when refining I1 freely might be compensated by protonation of the remaining phosphine moiety. Although the reaction that yielded the first crystal of **5b** was carried out under rigorously dry condition to prevent protonation of the phosphine, the redox reaction that led to the formation of the [IP(*o*-tol)₃]⁺-cation might very well have produced protons. All non-hydrogen

atoms were refined anisotropically. Hydrogen atoms were assigned to idealized geometric positions and included in structure factors calculations.

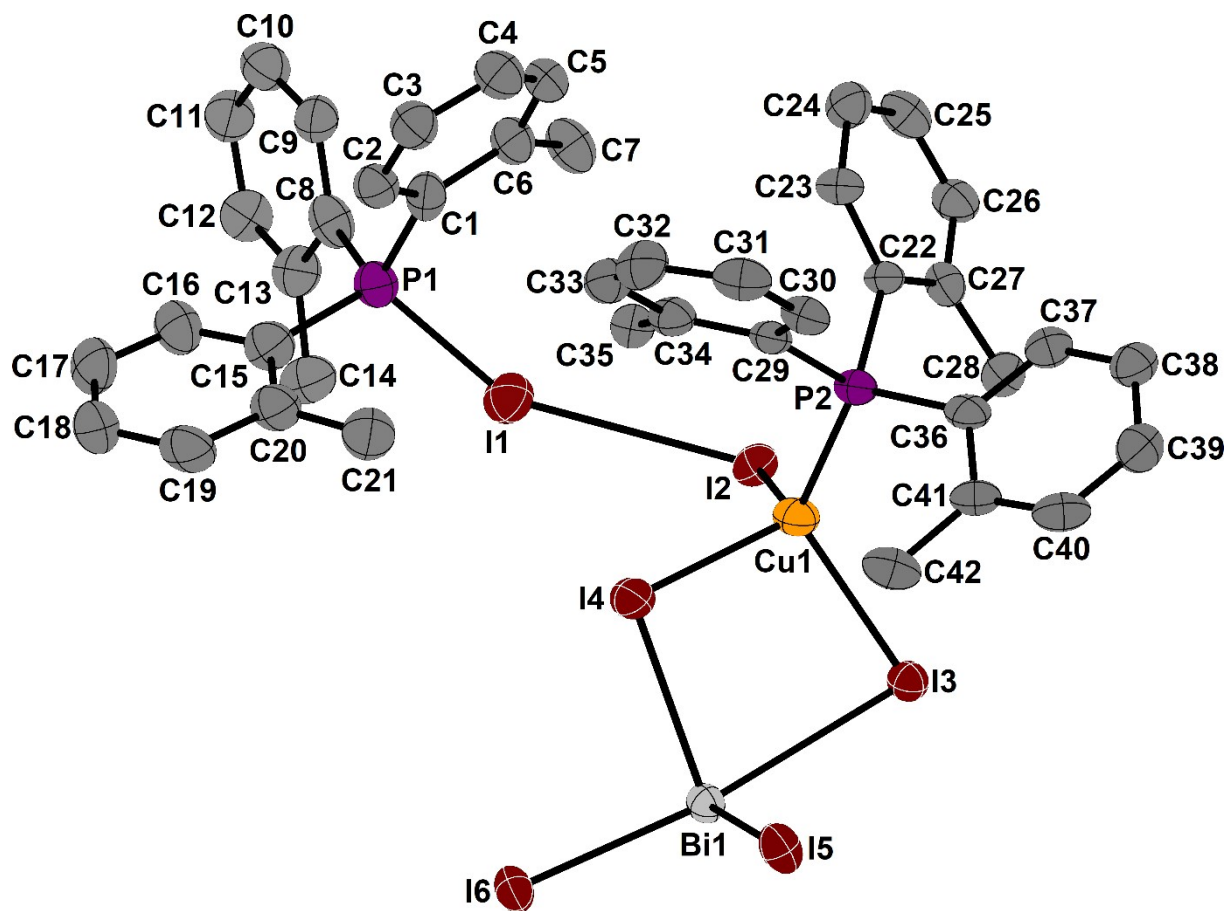


Figure S9: Asymmetric unit of **5b**, ellipsoids at 50 % probability. Hydrogen atoms are omitted for clarity.

Table S9: Crystallographic data for **6**, measured on a Bruker D8 Quest at 100 K, CCDC 2102773.

6	
Empirical formula	C ₈₄ H ₈₆ Ag ₂ I ₁₀ P ₄ Sb ₂
Formula weight	2947.64
Temperature/K	100.0
Crystal system	triclinic
Space group	<i>P</i> -1
<i>a</i> /Å	13.3248(5)
<i>b</i> /Å	14.3029(6)
<i>c</i> /Å	14.7856(6)
α /°	61.9970(10)
β /°	76.4210(10)
γ /°	66.4810(10)
Volume/Å ³	2277.38(16)
<i>Z</i>	1
ρ_{calc} /cm ³	2.149
μ /mm ⁻¹	4.510
Absorption correction (<i>T</i> _{min} / <i>T</i> _{max})	multi-scan (0.0654/ 0.0915)
<i>F</i> (000)	1376.0
Crystal size/mm ³	0.114 × 0.064 × 0.054
Radiation	MoK α (λ = 0.71073)
2 θ range for data collection/°	4.438 to 50.638
Index ranges	-16 ≤ <i>h</i> ≤ 16, -17 ≤ <i>k</i> ≤ 17, -17 ≤ <i>l</i> ≤ 17
Reflections collected	41912
Independent reflections	8277 [<i>R</i> _{int} = 0.0669, <i>R</i> _{sigma} = 0.0506]
Data/restraints/parameters	8277/0/466
Goodness-of-fit on <i>F</i> ²	1.088
Final <i>R</i> indexes [<i>I</i> ≥ 2 σ (<i>I</i>)]	<i>R</i> ₁ = 0.0438, <i>wR</i> ₂ = 0.0714
Final <i>R</i> indexes [all data]	<i>R</i> ₁ = 0.0675, <i>wR</i> ₂ = 0.0776
Largest diff. peak/hole / e Å ⁻³	2.05/-1.38

Details of crystal structure measurement and refinement: All non-hydrogen atoms were refined anisotropically. Hydrogen atoms were assigned to idealized geometric positions and included in structure factors calculations.

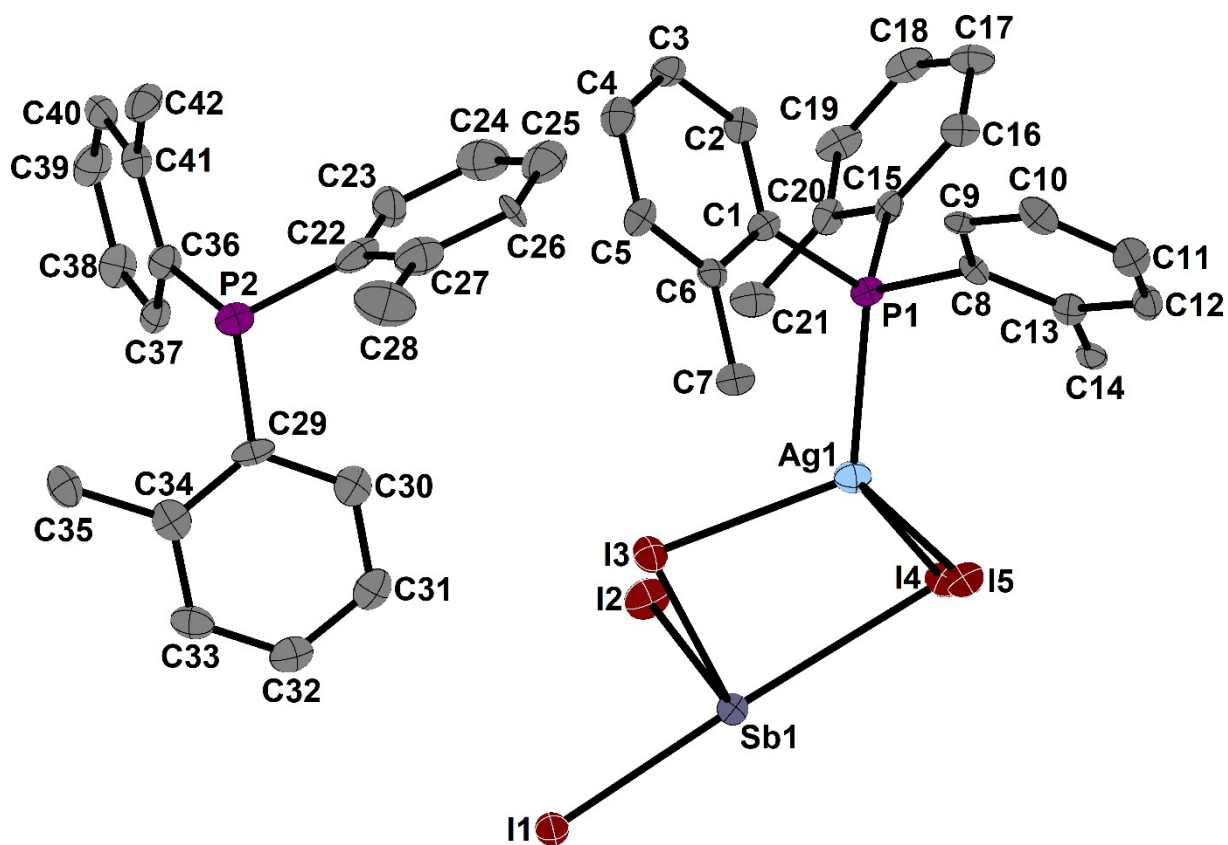


Figure S10: Asymmetric unit of **6**, ellipsoids at 50 % probability. Hydrogen atoms are omitted for clarity.

Table S10: Crystallographic data for **7**, measured on a Stoe IPDS2 at 100 K, CCDC 2102772.

7	
Empirical formula	C _{74.8} H _{64.2} Ag ₄ Bi ₂ I ₁₀ N _{1.4} P ₄
Formula weight	3224.99
Temperature/K	100.0
Crystal system	triclinic
Space group	<i>P</i> -1
<i>a</i> /Å	13.2600(10)
<i>b</i> /Å	14.3061(13)
<i>c</i> /Å	14.5411(11)
α /°	101.487(6)
β /°	108.303(6)
γ /°	115.047(6)
Volume/Å ³	2188.6(3)
<i>Z</i>	1
ρ_{calc} /cm ³	2.447
μ /mm ⁻¹	8.522
Absorption correction (<i>T</i> _{min} / <i>T</i> _{max})	numerical (0.2149/ 0.3016)
<i>F</i> (000)	1467.0
Crystal size/mm ³	0.25696 × 0.20024 × 0.18873
Radiation	MoK α (λ = 0.71073)
2 θ range for data collection/°	3.198 to 53.826
Index ranges	-16 ≤ <i>h</i> ≤ 16, -18 ≤ <i>k</i> ≤ 18, -18 ≤ <i>l</i> ≤ 18
Reflections collected	24200
Independent reflections	9283 [<i>R</i> _{int} = 0.0821, <i>R</i> _{sigma} = 0.0983]
Data/restraints/parameters	9283/2249/419
Goodness-of-fit on <i>F</i> ²	0.944
Final <i>R</i> indexes [<i>I</i> ≥ 2 σ (<i>I</i>)]	<i>R</i> ₁ = 0.0469, <i>wR</i> ₂ = 0.0944
Final <i>R</i> indexes [all data]	<i>R</i> ₁ = 0.1109, <i>wR</i> ₂ = 0.1132
Largest diff. peak/hole / e Å ⁻³	1.32/-1.82

Details of crystal structure measurement and refinement: The phenyl groups as well as the solvate acetonitrile molecule were modelled using the FragmentDB / DSR.² SADI, SIMU and RIGU restraints needed to be applied to the phenyl groups and DFIX restraints to the acetonitrile molecule to ensure a stable refinement. The acetonitrile molecule and two of the phenyl groups, which are disordered, were refined isotropically. All other non-hydrogen atoms were refined anisotropically. The occupancies of the acetonitrile molecule and the disordered phenyl groups were refined freely to 70 % for the acetonitrile group, to 58 % / 42% for phenyl groups 5 and 6 and 44 % / 56 % for phenyl groups 7 and 8 (see also figure S11). The shape of the ellipsoids of phenyl group 4 also suggests a disorder. However, it was not possible to model this group as two distinct parts. Hydrogen atoms were assigned to idealized geometric positions and included in structure factors calculations.

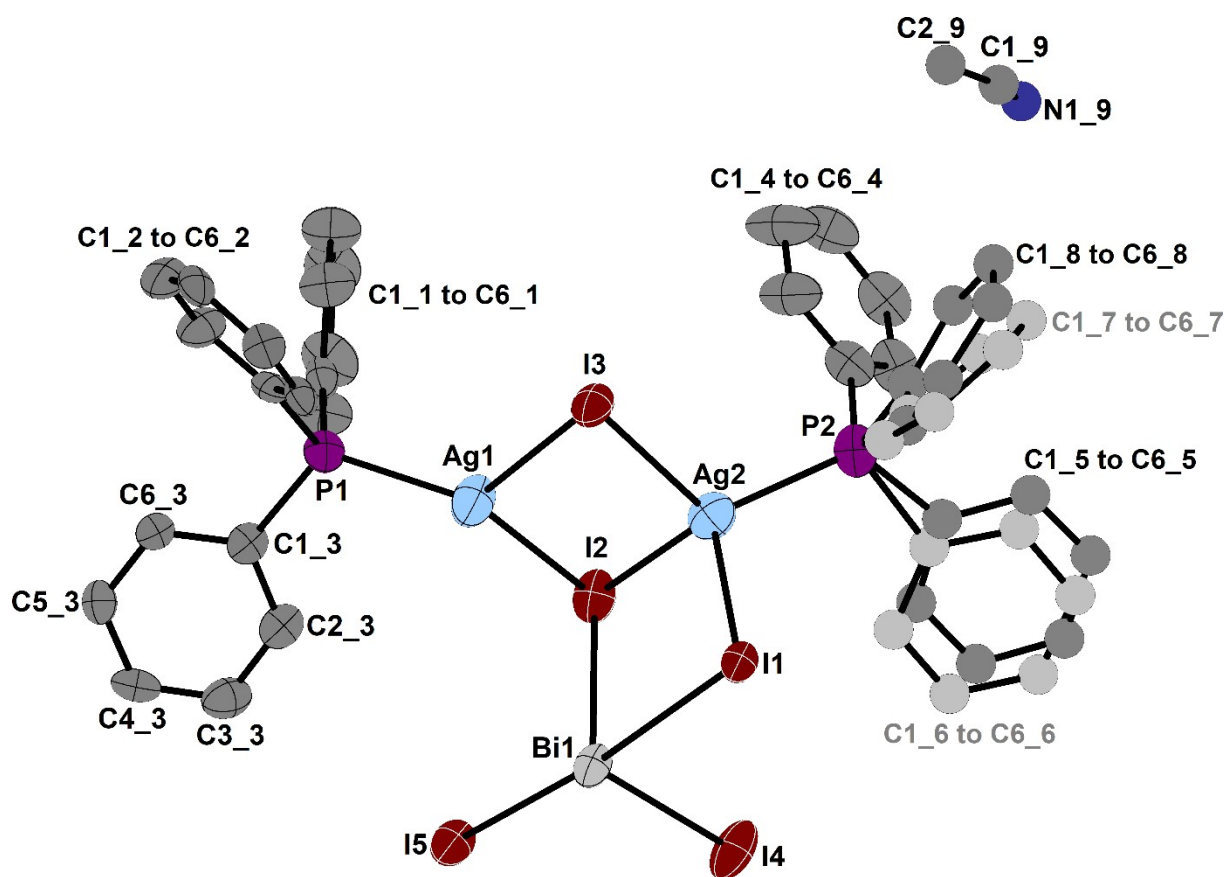


Figure S11: Asymmetric unit of **7**, ellipsoids at 50 % probability, isotropically refined atoms are shown as spheres with a diameter of 0.3 Å. Hydrogen atoms are omitted for clarity. All phenyl groups are named analogous to group 3. Less occupied parts of disordered phenyl groups are shown in a lighter color.

Additional crystal structures that are not discussed in the main article

In addition to the compounds discussed in the main article, we also obtained a number of different phosphonium iodido bismuthates and antimonates during our experiments as side products while exploring different reaction conditions. They do not give significant new insights into the topic at hand and their anionic motifs have been observed frequently already in the chemistry of iodido bismuthates and antimonates. So we include their single crystal structures here for the sake of completeness and to help other researchers who want to prepare multinary iodido bismuthates with arylphosphonium-cations. As all of these compounds are of lesser interest in the context of our search for new compounds with ternary anions, we did not optimize their synthesis. They generally crystallized within a few days to a few weeks from solutions of pentel iodides, coinage metal iodides and $P(R_3)$ in acetonitrile, acetone or 1,2-dimethoxyethane, which were dissolved by heating under reflux cooling for about one hour.

Table S11: Crystallographic data for **B**, measured on a Stoe StadiVari at 273 K, CCDC 2102786.

B	
Empirical formula	C ₆₈ H ₁₀₂ Bi ₂ Cu ₂ I ₁₀ N ₂ P ₂
Formula weight	2823.49
Temperature/K	273.0
Crystal system	orthorhombic
Space group	<i>Pbca</i>
a/Å	19.5215(6)
b/Å	18.4350(5)
c/Å	24.6449(5)
α/°	90
β/°	90
γ/°	90
Volume/Å ³	8869.2(4)
Z	4
ρ _{calc} /g/cm ³	2.115
μ/mm ⁻¹	36.117
Absorption correction (T _{min} /T _{max})	Multi-scan (0.0288/ 0.0952)
F(000)	5232.0
Crystal size/mm ³	0.04 × 0.037 × 0.037
Radiation	CuKα (λ = 1.54178)
2θ range for data collection/°	7.174 to 134.996
Index ranges	-23 ≤ h ≤ 21, -22 ≤ k ≤ 15, -29 ≤ l ≤ 27
Reflections collected	48412
Independent reflections	7962 [R _{int} = 0.0812, R _{sigma} = 0.0791]
Data/restraints/parameters	7962/308/390
Goodness-of-fit on F ²	0.748
Final R indexes [I ≥ 2σ (I)]	R ₁ = 0.0363, wR ₂ = 0.0755
Final R indexes [all data]	R ₁ = 0.0771, wR ₂ = 0.0873
Largest diff. peak/hole / e Å ⁻³	0.78/-0.86

Details of crystal structure measurement and refinement: The measurement needed to be carried out at 273 K due to splitting of the crystal upon cooling. The butyl groups of the cation are strongly disordered. For two of these groups (C5 to C8 and C13 to C16) this could be modelled as two distinct parts with occupancies of 60 % / 40 %. Atoms disordered over two parts were refined isotropically. All other non-hydrogen atoms were refined anisotropically. However the size and shape of the ellipsoids of the other two butyl groups suggests additional disorder. SADI restraints had to be used for all N-C and C-C bonds and angles in the NBu₄-moiety to ensure a stable refinement. RIGU restraints had to be used on the anisotropically refined butyl groups and additional DELU and SIMU restraints on one of the butyl groups and on one of the phenyl groups. Hydrogen atoms were assigned to idealized geometric positions and included in structure factors calculations.

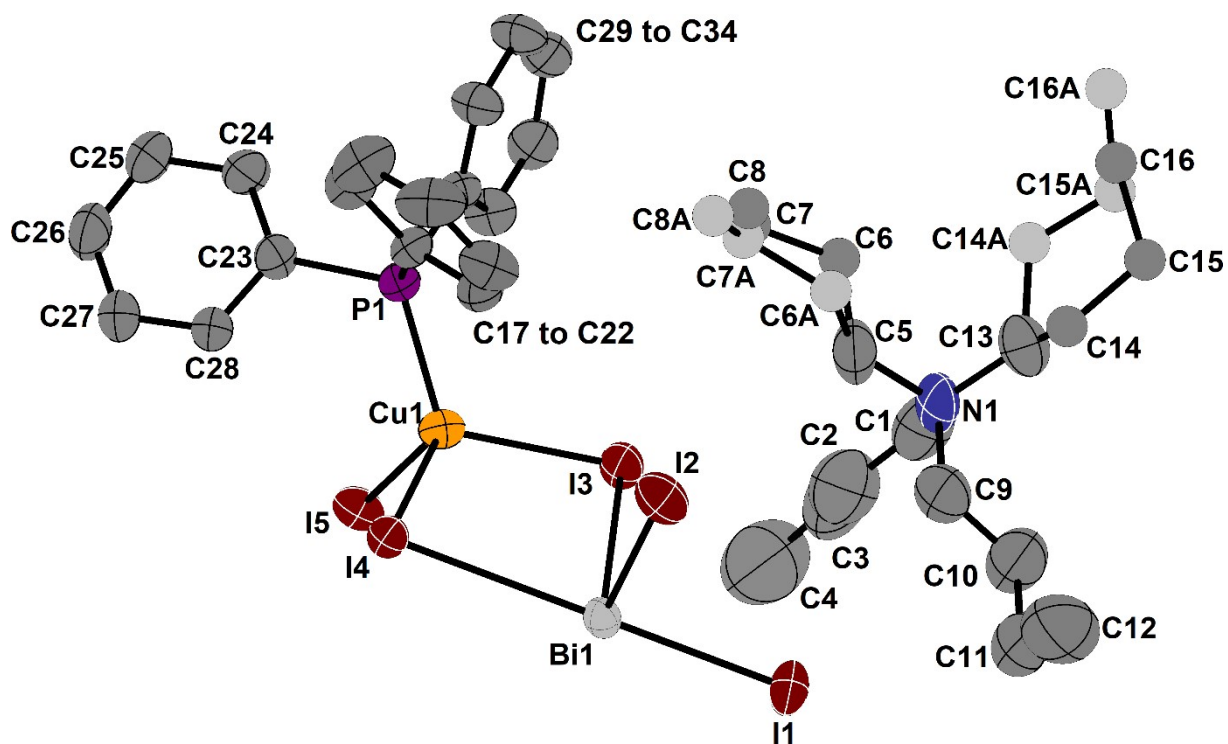


Figure S12: Asymmetric unit of **B**, ellipsoids at 30 % probability, isotropically refined atoms are shown as spheres with a diameter of 0.3 Å. Hydrogen atoms are omitted for clarity. Less occupied parts of disordered butyl groups are shown in a lighter color.

Table S12: Crystallographic data for **C**, measured on a Stoe StadiVari at 100 K, CCDC 2102779.

C	
Empirical formula	Ag ₃ Bi ₇ C ₂₅₆ H ₂₁₈ I ₂₆ N ₂ P ₁₄
Formula weight	8841.76
Temperature/K	100.0
Crystal system	tetragonal
Space group	<i>P4₂/n</i>
a/Å	30.5142(3)
b/Å	30.5142(3)
c/Å	28.9299(3)
α/°	90
β/°	90
γ/°	90
Volume/Å ³	26937.1(6)
Z	4
ρ _{calc} /g/cm ³	2.160
μ/mm ⁻¹	35.045
Absorption correction (T _{min} /T _{max})	Multi-scan (0.0012/ 0.0063)
F(000)	16136.0
Crystal size/mm ³	0.0929 × 0.0687 × 0.06346
Radiation	CuKα (λ = 1.54186)
2θ range for data collection/°	6.11 to 152.61
Index ranges	-25 ≤ h ≤ 37, -38 ≤ k ≤ 26, -36 ≤ l ≤ 24
Reflections collected	143624
Independent reflections	26636 [R _{int} = 0.0622, R _{sigma} = 0.0925]
Data/restraints/parameters	26636/16255/1357
Goodness-of-fit on F ²	0.820
Final R indexes [I ≥ 2σ (I)]	R ₁ = 0.0395, wR ₂ = 0.0662
Final R indexes [all data]	R ₁ = 0.0887, wR ₂ = 0.0748
Largest diff. peak/hole / e Å ⁻³	1.03/-0.90

Details of crystal structure measurement and refinement: All phenyl groups were modelled using the FragmentDB / DSR.² SADI, SIMU and RIGU restraints needed to be applied to the phenyl groups to ensure a stable refinement. Additionally ISOR restraints needed to be applied to some of the carbon atoms. One of the phenyl group is disordered and was modelled as two parts (groups 21 and 22), which were refined isotropically. The occupancies of the two parts were refined freely to 53 % / 47% for groups 21 and 22, respectively (see also figure S13). All other non-hydrogen atoms were refined anisotropically. The shape of the ellipsoids of phenyl group 15 also suggests a disorder. However, it was not possible to model this group as two distinct parts. Additionally solvent accessible voids were found in the structure and assigned two molecules of MeCN using a solvent mask. Hydrogen atoms were assigned to idealized geometric positions and included in structure factors calculations.

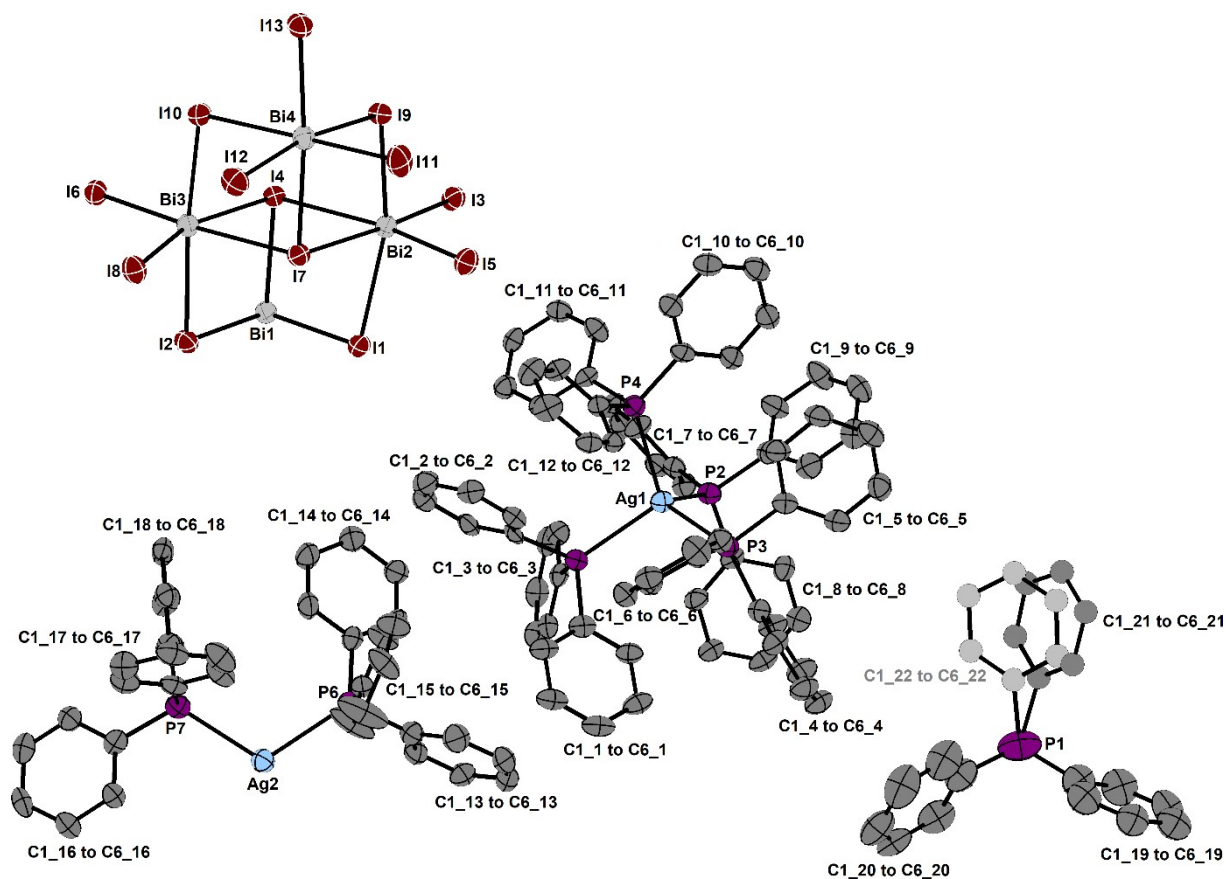


Figure S13: Asymmetric unit of **C**, ellipsoids at 50 % probability, isotropically refined atoms are shown as spheres with a diameter of 0.3 Å. Hydrogen atoms are omitted for clarity. Less occupied part of the disordered phenyl group is shown in a lighter color.

Table S13: Crystallographic data for **D**, measured on a Stoe IPDS2 at 100 K, CCDC 2102777.

D	
Empirical formula	C ₁₀₅ H ₁₀₉ Bi ₃ I ₁₁ O ₆ P ₅
Formula weight	3644.61
Temperature/K	100.0
Crystal system	triclinic
Space group	<i>P</i> -1
<i>a</i> /Å	14.3764(3)
<i>b</i> /Å	14.5247(3)
<i>c</i> /Å	28.6661(6)
α /°	75.574(2)
β /°	85.461(2)
γ /°	86.580(2)
Volume/Å ³	5774.0(2)
<i>Z</i>	2
ρ_{calc} /cm ³	2.096
Absorption correction (<i>T</i> _{min} / <i>T</i> _{max})	numerical (0.2849/ 0.7750)
<i>F</i> (000)	3388.0
Crystal size/mm ³	0.31965 × 0.0636 × 0.06105
Radiation	MoK α (λ = 0.71073)
2 θ range for data collection/°	2.844 to 53.634
Index ranges	-18 ≤ <i>h</i> ≤ 18, -17 ≤ <i>k</i> ≤ 18, -36 ≤ <i>l</i> ≤ 36
Reflections collected	24339
Independent reflections	24339 [<i>R</i> _{merge} = 0.2589, <i>R</i> _{sigma} = 0.0605, <i>R</i> _{int} = 0.0821 (not de-twinning data)]
Data/restraints/parameters	24339/11198/1255
Goodness-of-fit on <i>F</i> ²	1.066
Final <i>R</i> indexes [<i>I</i> ≥ 2 σ (<i>I</i>)]	<i>R</i> ₁ = 0.0630, <i>wR</i> ₂ = 0.1769
Final <i>R</i> indexes [all data]	<i>R</i> ₁ = 0.0861, <i>wR</i> ₂ = 0.1911
Largest diff. peak/hole / e Å ⁻³	3.16/-3.69

Details of crystal structure measurement and refinement: The crystal was non-merohedrally twinned after (-0.01, 0.99, 0, 1.01, 0.01, 0, 0.616, 0.616, -1). Initial structure solution and refinement was performed on the complete dataset. The large number of residue electron density peaks that is not associated with heavy elements suggests that additional twin domains may be present. However we were not able to de-twin the data further.

One of the *ortho*-tolyl groups is disordered and was modelled as two parts with occupancies of 56 % and 44 %. All non-hydrogen atoms were refined anisotropically. Hydrogen atoms were assigned to idealized geometric positions and included in structure factors calculations.

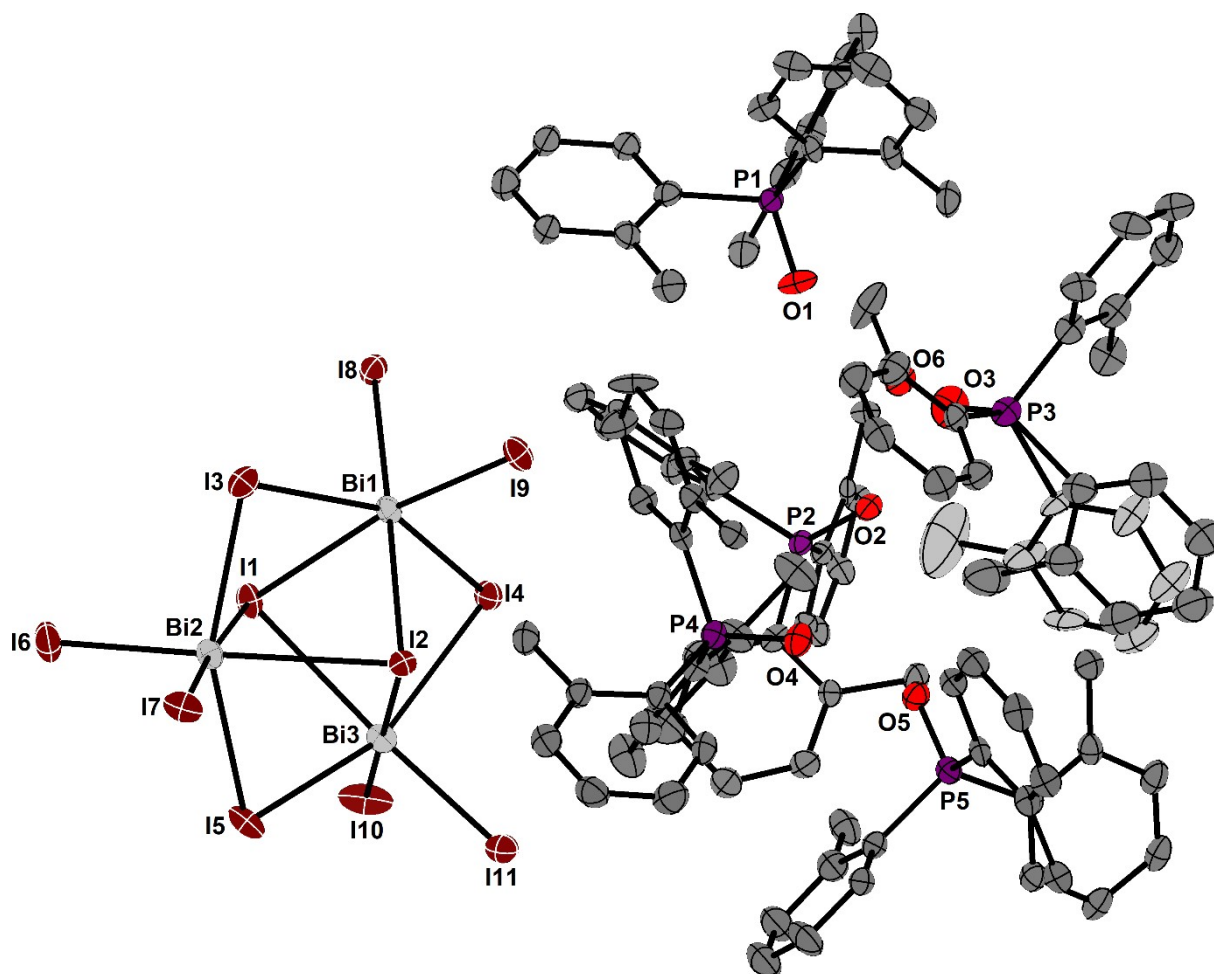


Figure S14: Asymmetric unit of **D**, ellipsoids at 50 % probability. Hydrogen atoms and labels of carbon atoms are omitted for clarity. Less occupied part of the disordered *ortho*-tolyl group is shown in a lighter color.

Table S14: Crystallographic data for **E**, measured on a Stoe StadiVari at 263 K, CCDC 2102776.

	E
Empirical formula	C ₇₅ H ₈₂ Cu ₂ I ₁₅ N ₆ P ₃ Sb ₄
Formula weight	3677.99
Temperature/K	263
Crystal system	trigonal
Space group	<i>R</i> -3
a/Å	14.9522(8)
b/Å	14.9522(8)
c/Å	82.431(9)
α/°	90
β/°	90
γ/°	120
Volume/Å ³	15960(2)
Z	5.99994
ρ _{calc} /g/cm ³	2.296
Absorption correction (T _{min} /T _{max})	multi-scan (0.0133/ 0.1239)
F(000)	10056.0
Crystal size/mm ³	0.193 × 0.178 × 0.13
Radiation	CuKα (λ = 1.54186)
2θ range for data collection/°	6.91 to 152.71
Index ranges	-16 ≤ h ≤ 18, -18 ≤ k ≤ 11, -103 ≤ l ≤ 94
Reflections collected	61987
Independent reflections	7419 [R _{int} = 0.1203, R _{sigma} = 0.1178]
Data/restraints/parameters	7419/0/321
Goodness-of-fit on F ²	0.693
Final R indexes [I ≥ 2σ (I)]	R ₁ = 0.0560, wR ₂ = 0.1143
Final R indexes [all data]	R ₁ = 0.1379, wR ₂ = 0.1425
Largest diff. peak/hole / e Å ⁻³	0.89/-0.41

Details of crystal structure measurement and refinement: The data was very weak, which resulted in a very low ratio of unique / observed reflections and—in combination with the high measurement temperature of 263 K—in a low precision on C-C bond length. All non-hydrogen atoms were refined anisotropically. Hydrogen atoms were assigned to idealized geometric positions and included in structure factors calculations.

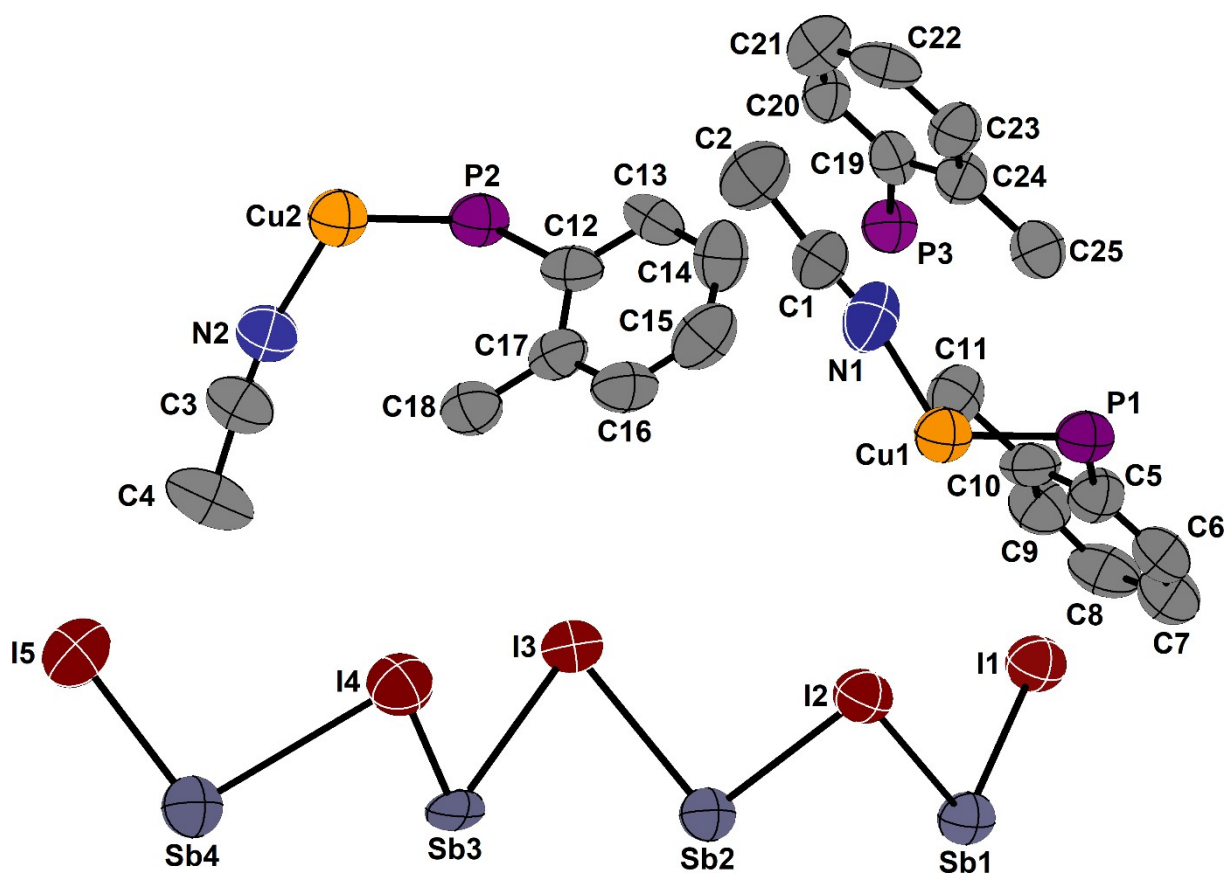


Figure S15: Asymmetric unit of E, ellipsoids at 30 % probability. Hydrogen atoms are omitted for clarity.

Thermal analysis

The thermal behavior of **1a** (16.1 mg), was studied by TGA/DSC on a NETSCH STA 409 C/CD from 25 °C to 1000 °C with a heating rate of 10 °C min⁻¹ in a constant flow of 80 ml min⁻¹ N₂ (see figure S16).

The sample shows one large mass loss of 78.3 % between 200 °C and 500 °C. This corresponds well to the evaporation of everything but CuI (theoretical value: 80.2 %). The beginning of this mass loss is accompanied by a sharp endothermic peak in the DSC-data at 222 °C, most likely is caused by the melting of the sample. Between 500 °C and 950 °C a second mass loss of 16.9 % is observed. The residue was identified as elemental copper *via* PXRD (see figure S35).

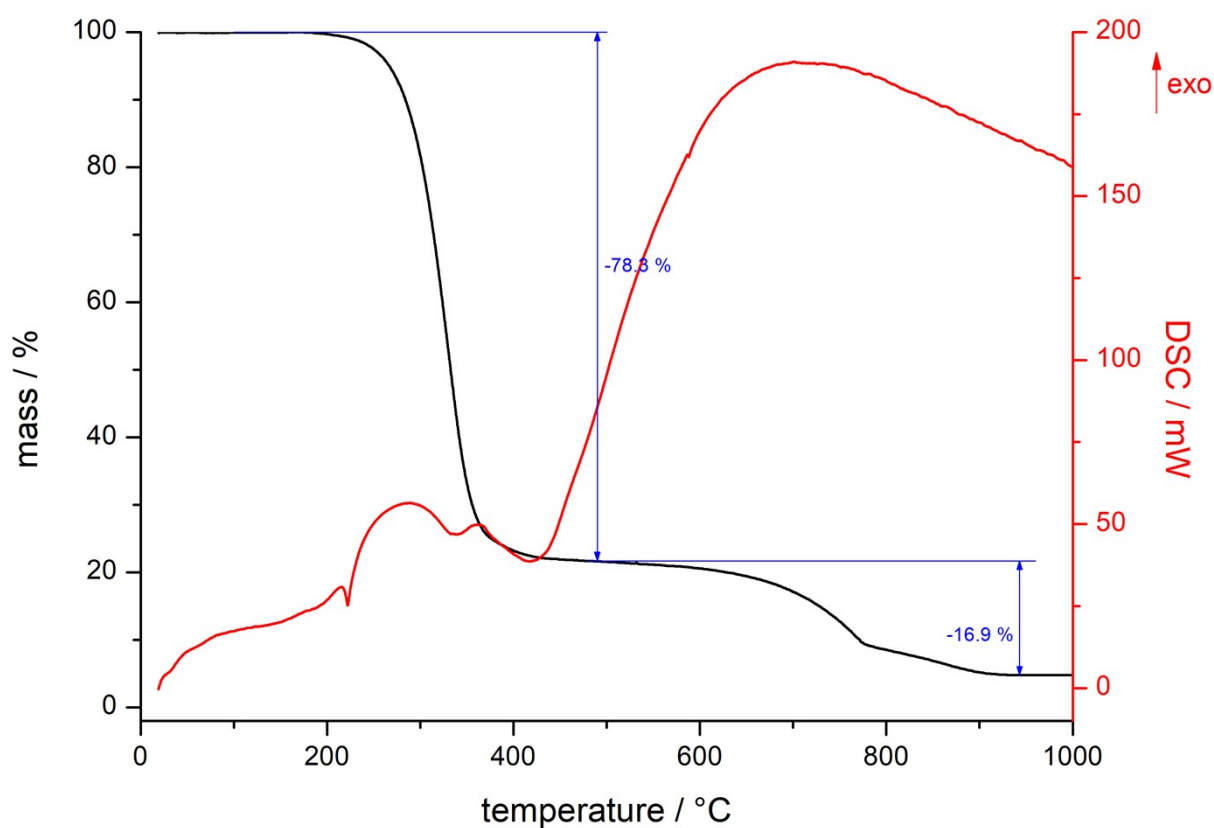


Figure S16. TGA/DSC of **1a**.

The thermal behavior of **2a** (18.4 mg), was studied by TGA/DSC on a NETSCH STA 409 C/CD from 25 °C to 1000 °C with a heating rate of 10 °C min⁻¹ in a constant flow of 80 ml min⁻¹ N₂ (see figure S17).

The sample shows a first mass loss between 90 °C and 150 °C of 6.6 %. This corresponds well to the spitting off of the acetonitrile ligands (theoretical value: 6.4 %). This process is accompanied by a broad endothermic peak in the DSC-data at 124 °C. The main decomposition occurs between 150 °C and 500 °C where additional 79.3 % of the initial sample mass are lost leaving a residue of 14.1 %. This corresponds well to the residue being CuI (theoretical value: 13.3 %). After a third mass loss up to 950 °C the final residue was identified as elemental copper *via* PXRD (see figure S36).

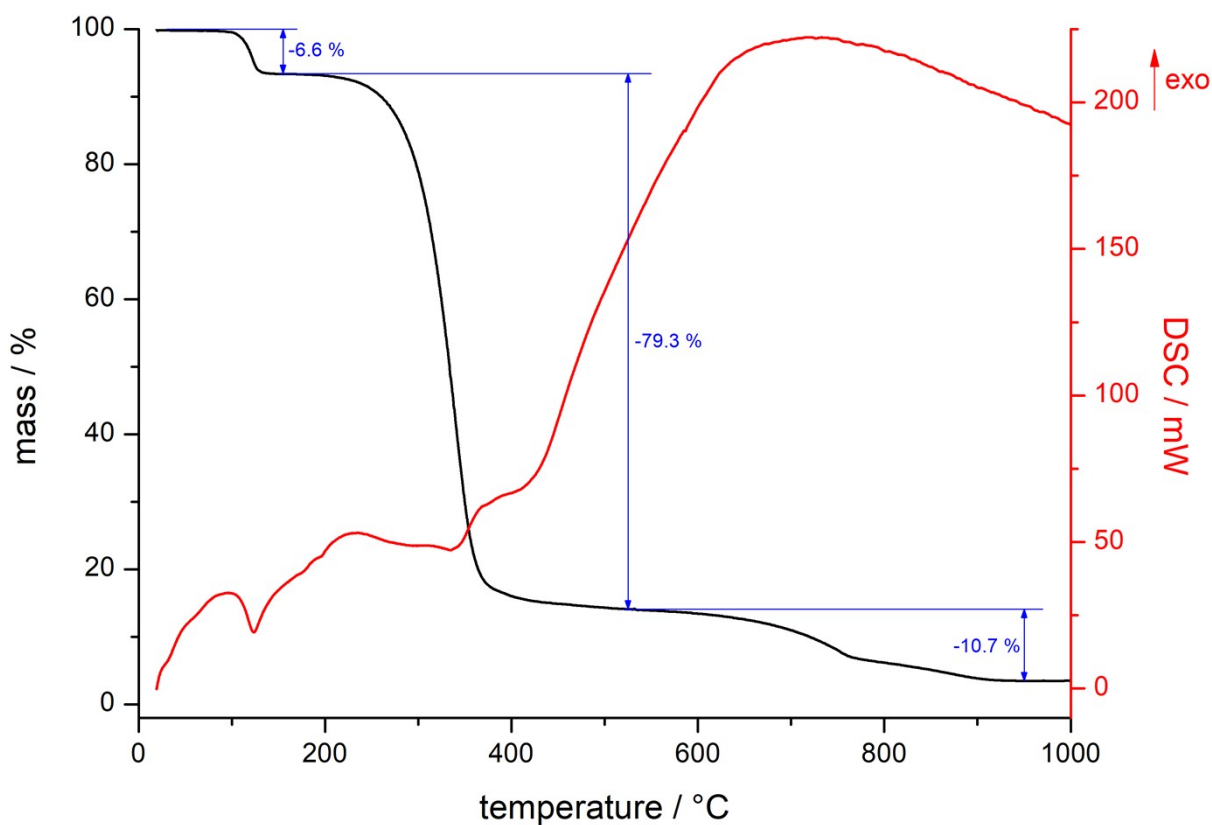


Figure S17. TGA/DSC of **2a**.

The thermal behavior of **2b** (16.6 mg), was studied by TGA/DSC on a NETSCH STA 409 C/CD from 25 °C to 1000 °C with a heating rate of 10 °C min⁻¹ in a constant flow of 80 ml min⁻¹ N₂ (see figure S18).

The sample shows a first mass loss between 120 °C and 170 °C of 5.6 %. This corresponds well to the spilling off of the acetonitrile ligands (theoretical value: 6.0 %). This process is accompanied by a broad endothermic peak in the DSC-data at 147 °C. The main decomposition occurs between 200 °C and 600 °C followed directly by a third step that continues up to the 1000 °C where the measurement was stopped leaving a residue of 6.0 %. At the start of the main decomposition step the DSC data shows another sharp endothermic peak at 212 °C. The residue at the end was identified as elemental copper and a small amount of Cu₃P *via* PXRD (see figure S37)

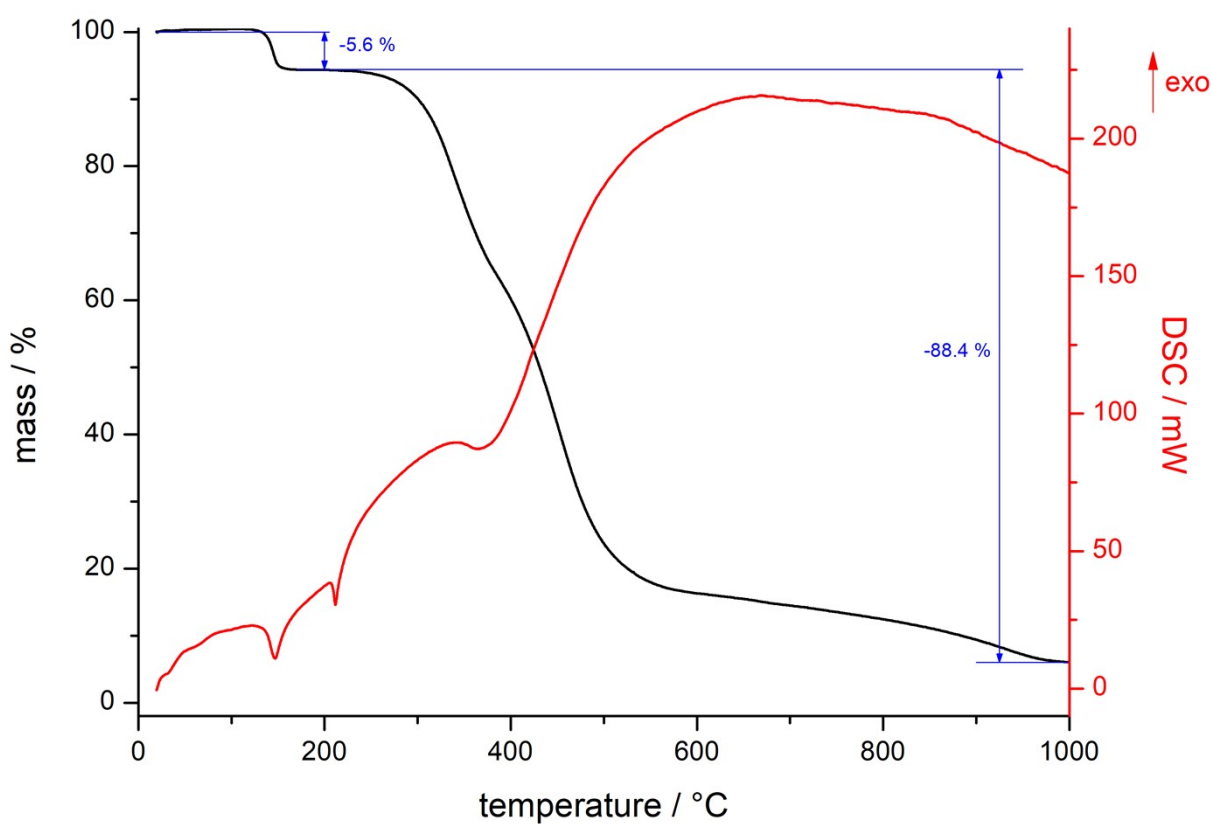


Figure S18. TGA/DSC of **2b**.

The thermal behavior of **4** (14.5 mg), was studied by TGA/DSC on a Mettler Toledo TGA-DSC 3 from 25 °C to 1000 °C with a heating rate of 10 °C min⁻¹ in a constant flow of 30 ml min⁻¹ N₂ (see figure S19).

The sample shows a first mass loss between 130 °C and 190 °C of 4.1 %. This corresponds well to the spiltting off of the acetone ligand (theoretical value: 3.5 %). The main decomposition occurs between 190 °C and 440 °C where 70.8 % of the mass are lost and is accompanied by a sharp peak in the DSC-data at 228 °C. This fits well to the evaporation of everything but CuI (theoretical value: 76.7 % overall mass loss). This decomposition is followed directly by a third step that continues up to about 800 °C.

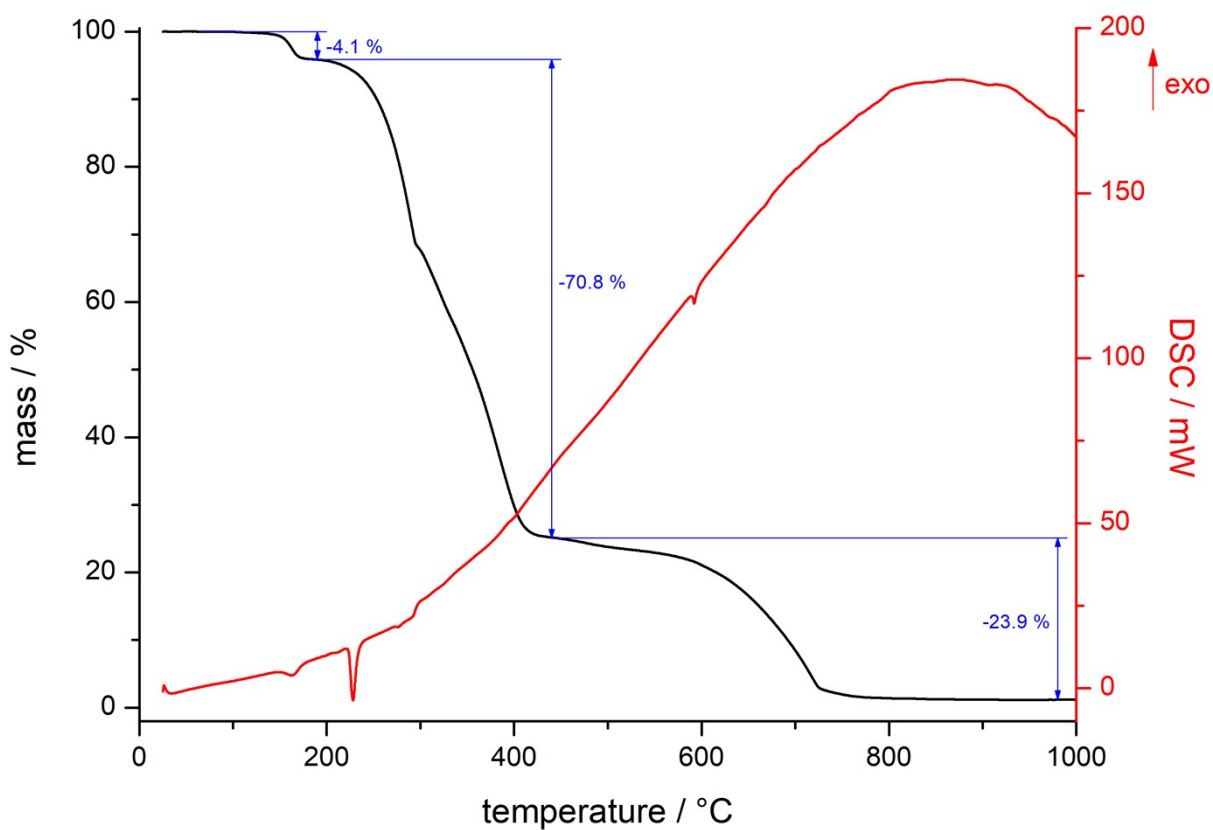


Figure S19. TGA/DSC of **4**.

The thermal behavior of **5a** (11.1 mg), was studied by TGA/DSC on a Mettler Toledo TGA-DSC 3 from 25 °C to 1000 °C with a heating rate of 10 °C min⁻¹ in a constant flow of 30 ml min⁻¹ N₂ (see figure S20).

The sample decomposes in one large complex step starting around 150 °C. It can be roughly divided into two parts of 84 % and 15 % at 480 °C. The beginning of this mass loss is accompanied by a sharp endothermic peak in the DSC-data at 229 °C, most likely is caused by the melting of the sample. The residue was identified to contain elemental copper and Cu₃P, *via* PXRD (see figure S38).

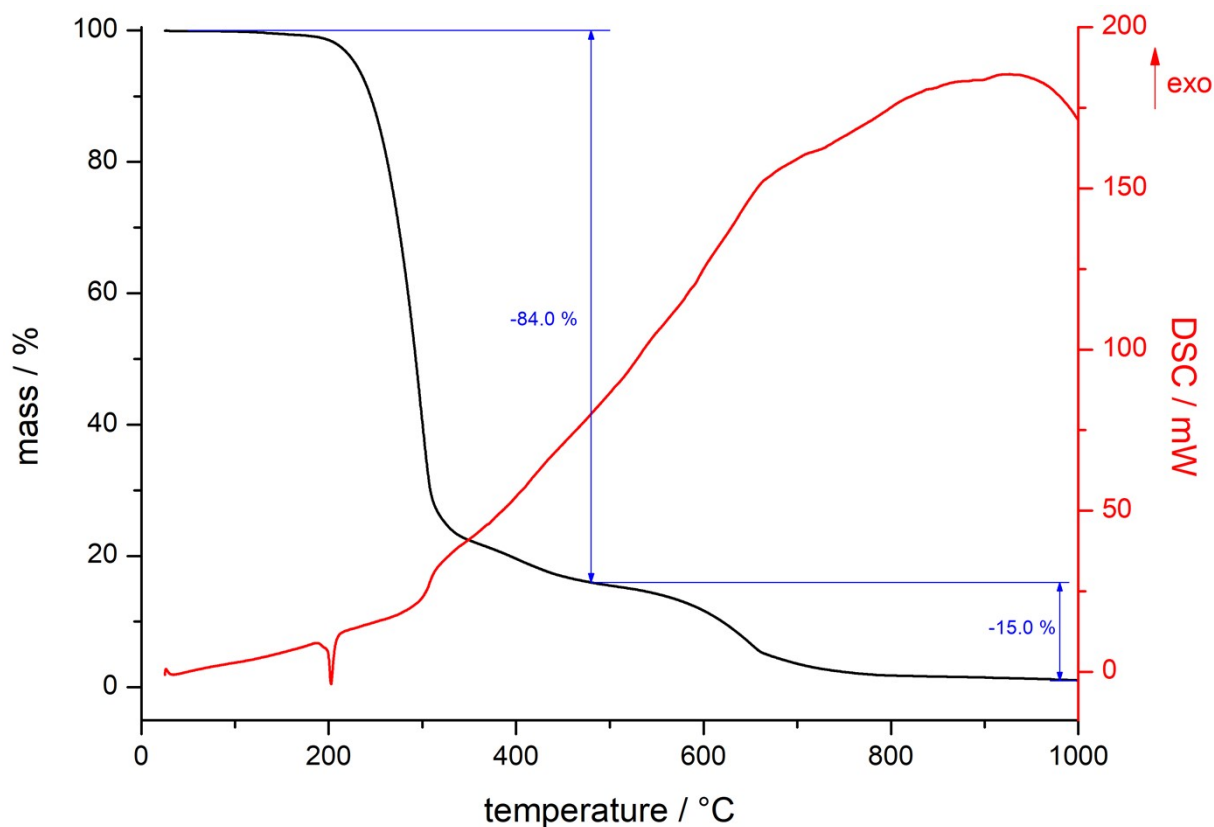


Figure S20. TGA/DSC of **5a**.

The thermal behavior of **5b** (12.4 mg), was studied by TGA/DSC on a Mettler Toledo TGA-DSC 3 from 25 °C to 1000 °C with a heating rate of 10 °C min⁻¹ in a constant flow of 30 ml min⁻¹ N₂ (see figure S21).

The sample behaves very similar to **5a**. It decomposes in one large complex step starting around 150 °C. It can be roughly divided into two parts of 84.7 % and 15.3 % at 470 °C. The beginning of this mass loss is accompanied by a sharp endothermic peak in the DSC-data at 231 °C, most likely is caused by the melting of the sample.

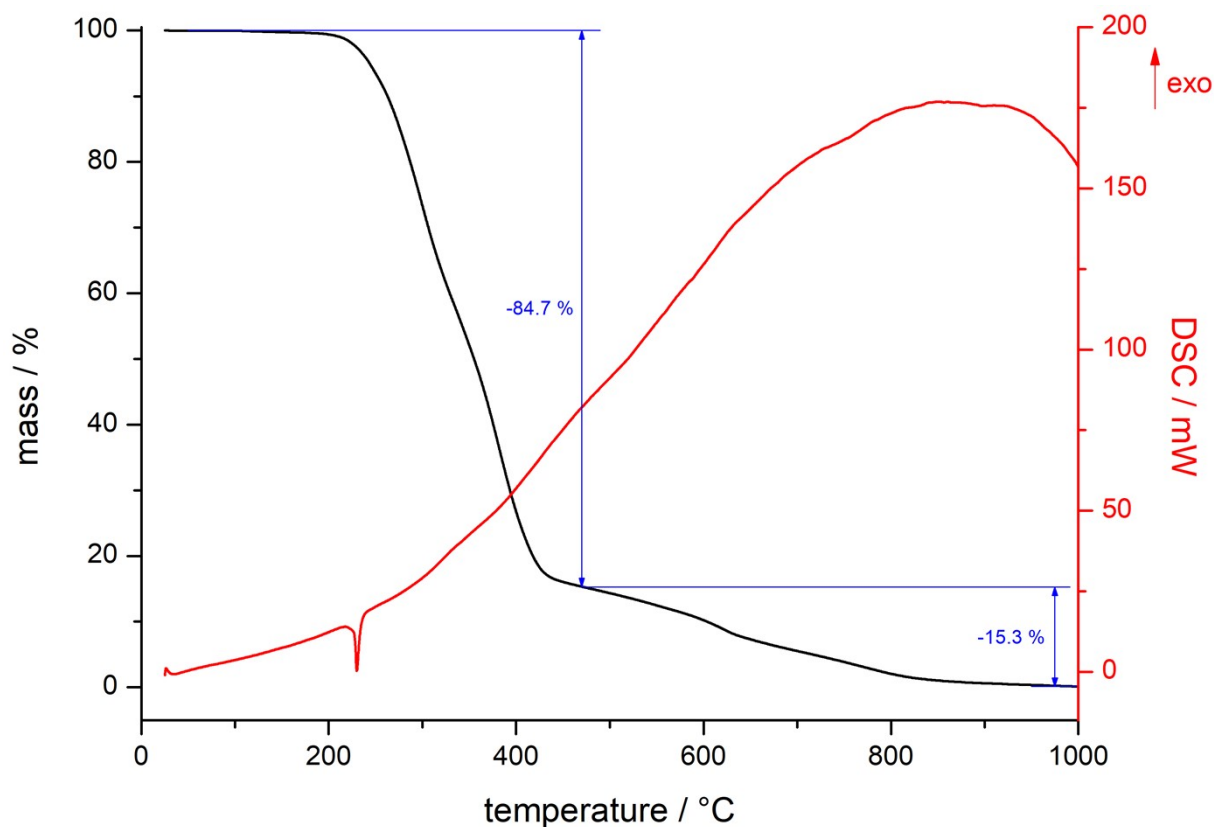


Figure S21. TGA/DSC of **5b**.

The thermal behavior of **6** (12.64 mg), was studied by TGA/DSC on a NETSCH STA 409 C/CD from 25 °C to 1000 °C with a heating rate of 10 °C min⁻¹ in a constant flow of 30 ml min⁻¹ N₂ (see figure S22).

The sample decomposes in one large step of 81.6 % between 160 °C and 460 C. This corresponds well to the evaporation of everything but AgI (theoretical value: 84.0 %). The beginning of this mass loss is accompanied by a sharp endothermic peak in the DSC-data at 168 °C, most likely is caused by the melting of the sample.

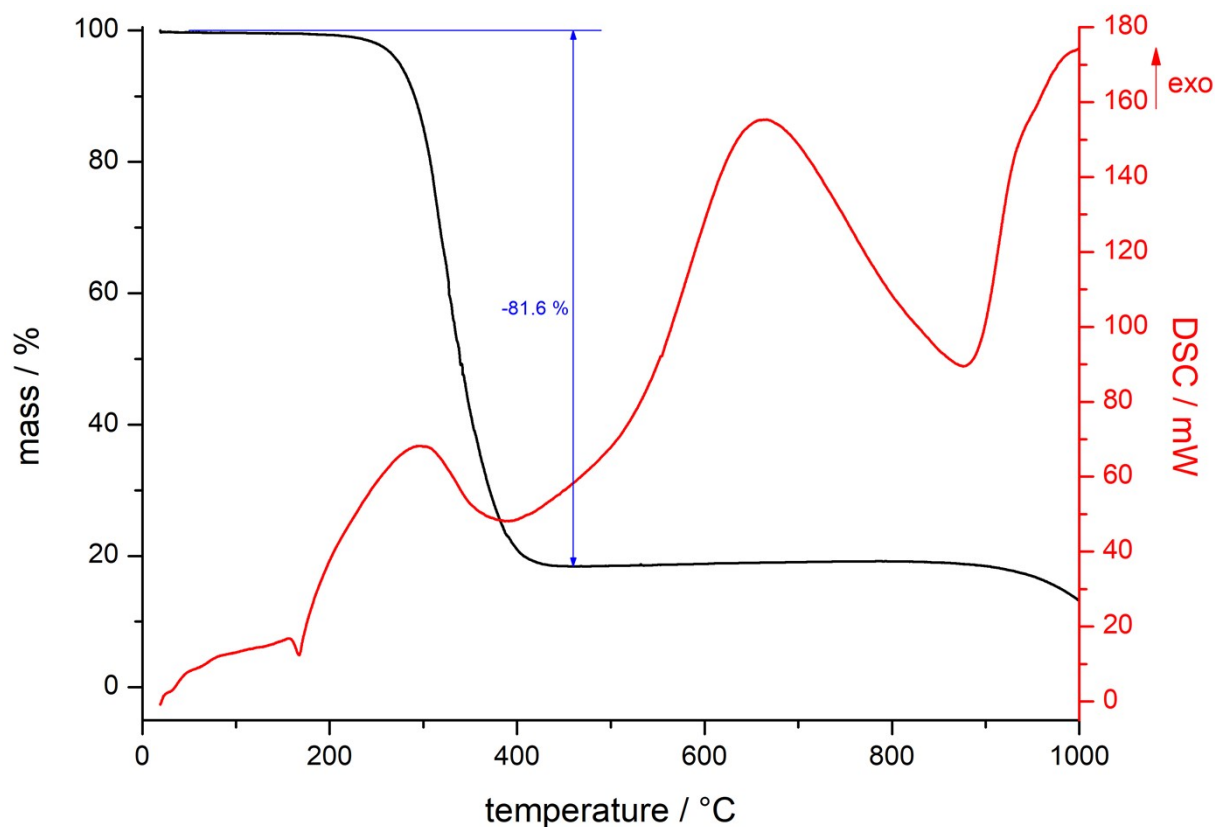


Figure S22. TGA/DSC of **6**.

Optical properties

Optical absorption spectra were recorded on a *Varian Cary 5000* UV/Vis/NIR spectrometer in the range of 400-800 nm in diffuse reflectance mode employing a *Praying Mantis* accessory (*Harrick*) with automatic baseline correction.

To determine the optical band gaps the raw data was transformed from reflectance R to absorption according to the Kubelka-Munk function

$$F(R) = \frac{(1 - R)^2}{2R}$$

and then plotted as a Tauc-plot, where $(F(R) \cdot h\nu)^{1/n}$ is plotted against radiation energy. For a direct band gap n would be $\frac{1}{2}$, for an indirect band gap $n = 2, 3, 4$. Since the transition in the region of interest was generally far more pronounced when choosing $n = \frac{1}{2}$, we assume that all analysed substances feature an indirect band gap.

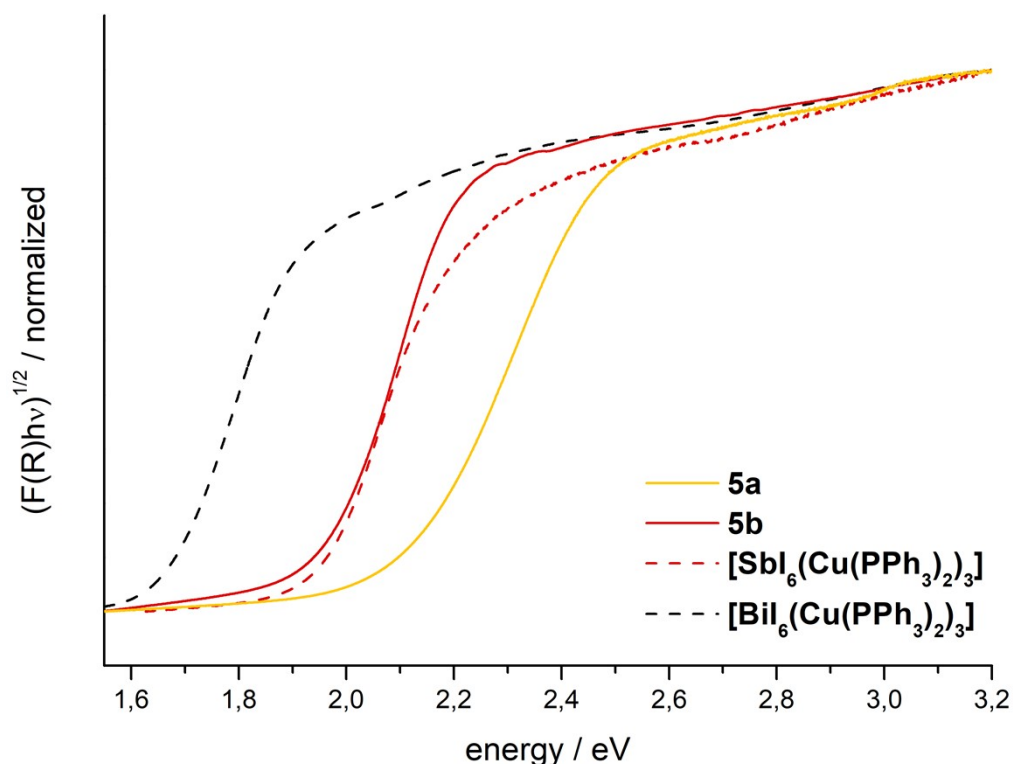


Figure S23. Tauc-plots from diffuse reflection UV-vis data, comparison of **5a/b** and $[\text{E}I_6(\text{Cu}(\text{PPh}_3)_2)_3]$.

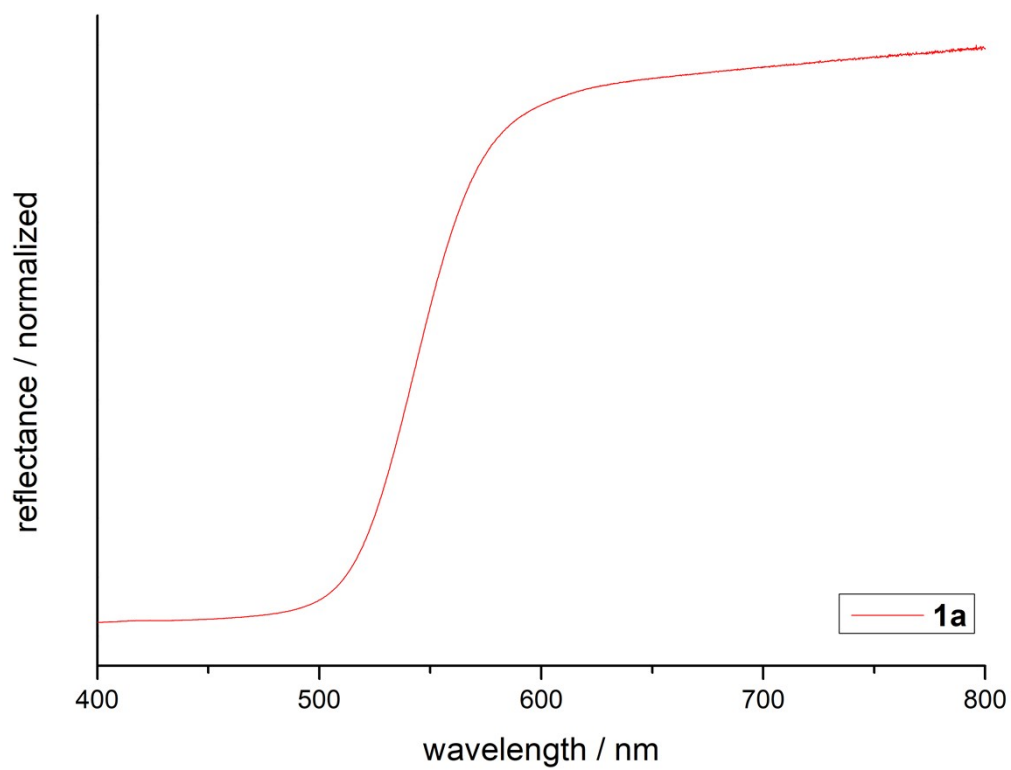


Figure S24. Raw UV-vis data of **1a**.

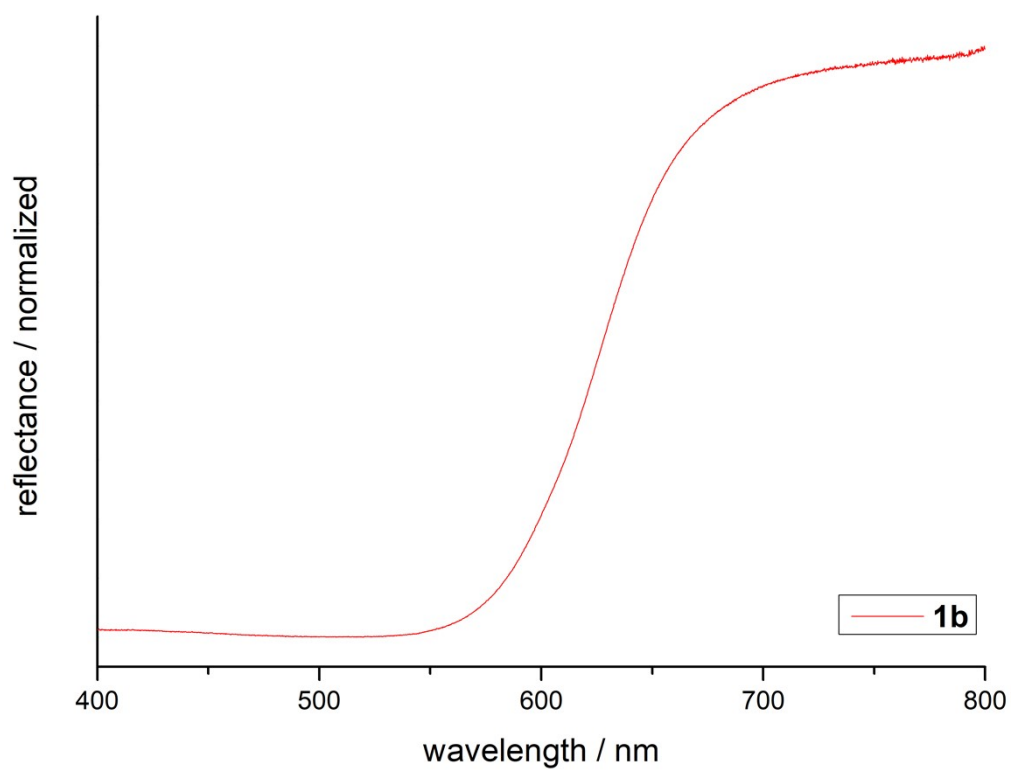


Figure S25. Raw UV-vis data of **1b**.

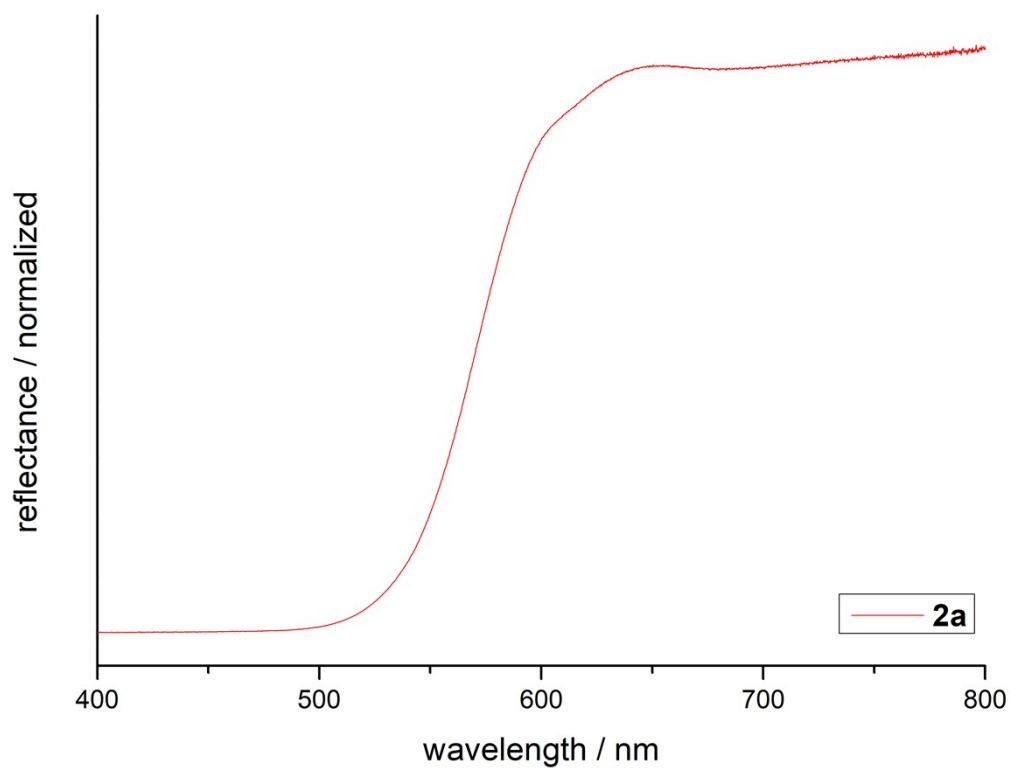


Figure S26. Raw UV-vis data of **2a**.

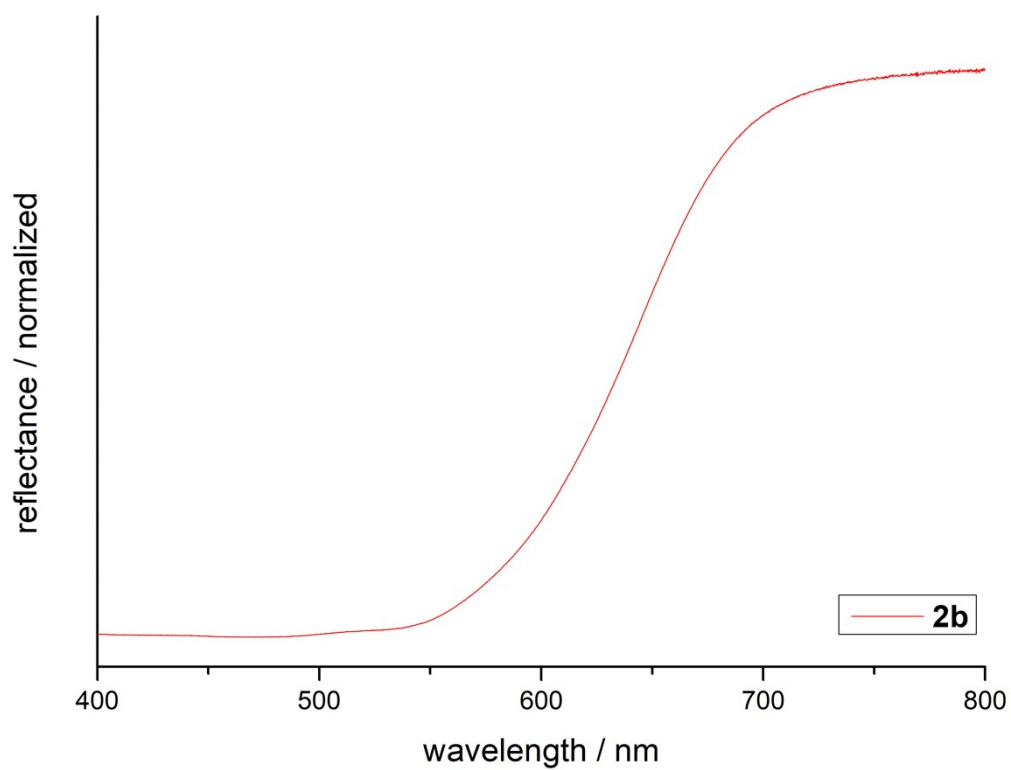


Figure S27. Raw UV-vis data of **2b**.

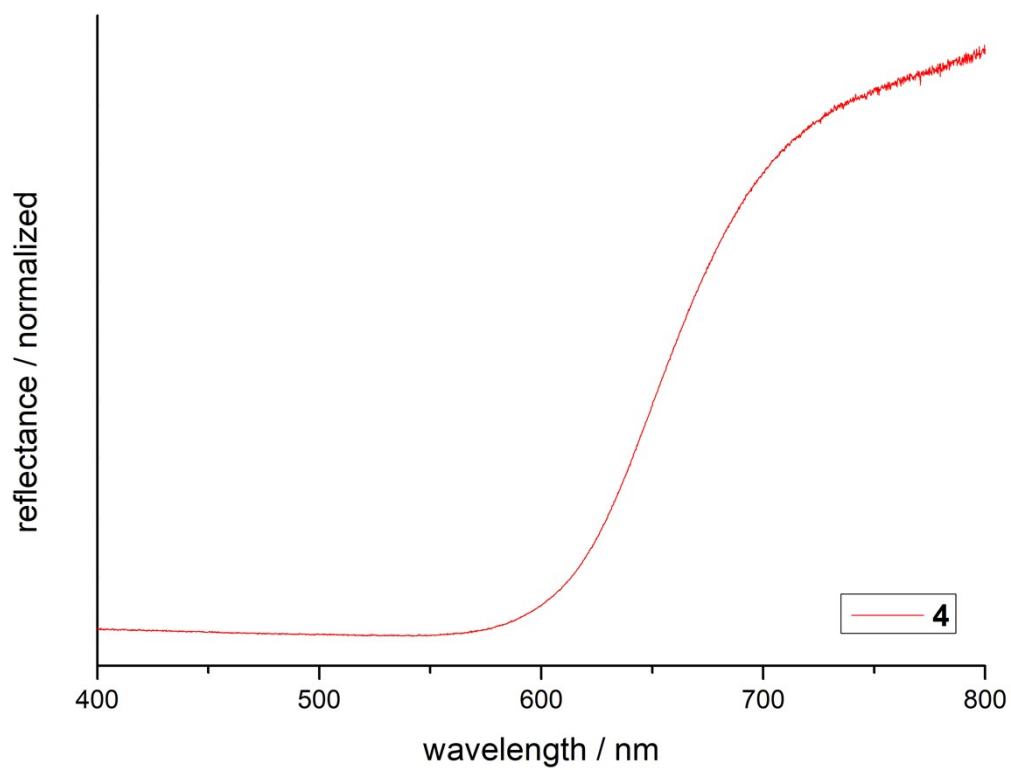


Figure S28. Raw UV-vis data of 4.

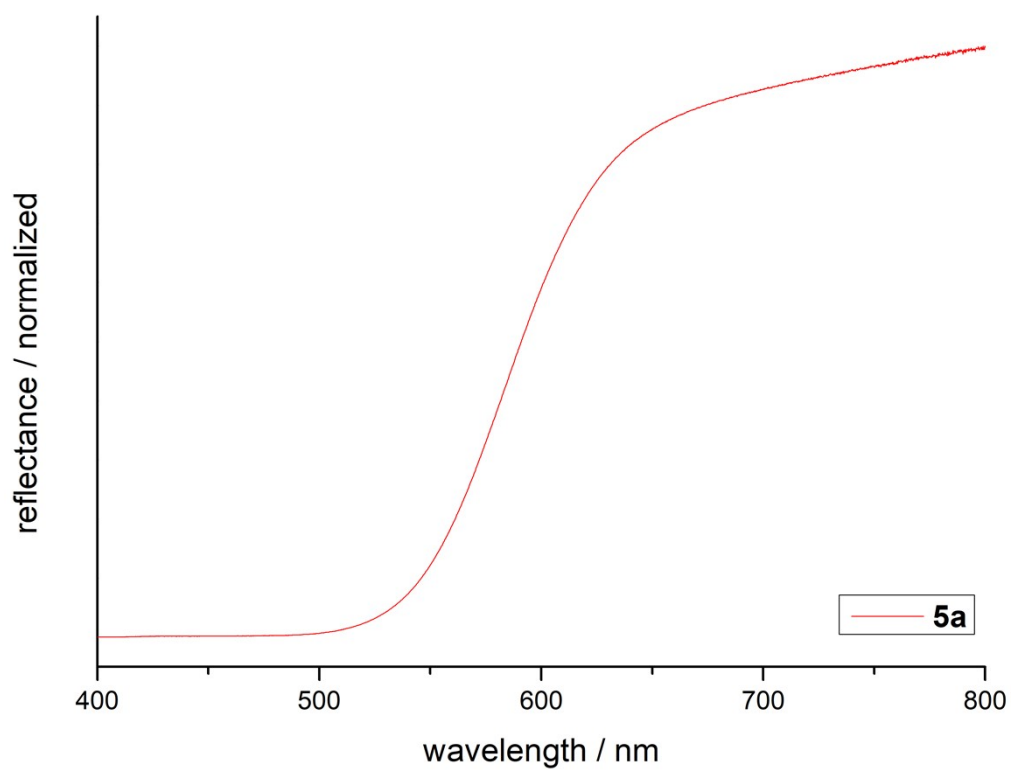


Figure S29. Raw UV-vis data of 5a.

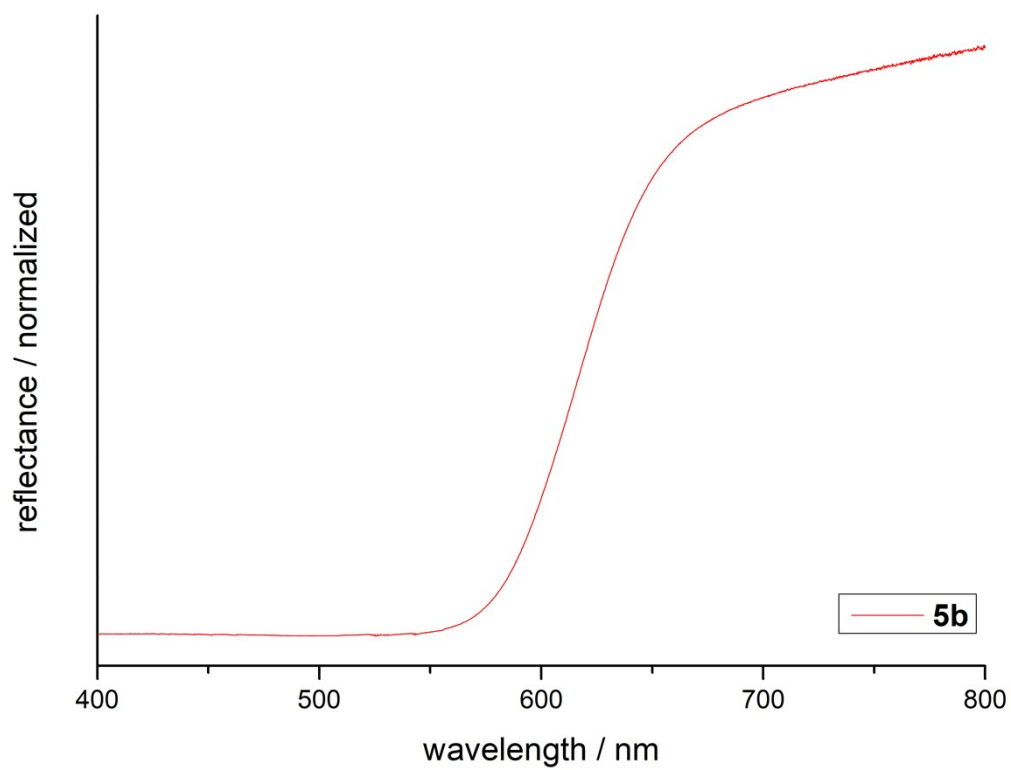


Figure S30. Raw UV-vis data of **5b**.

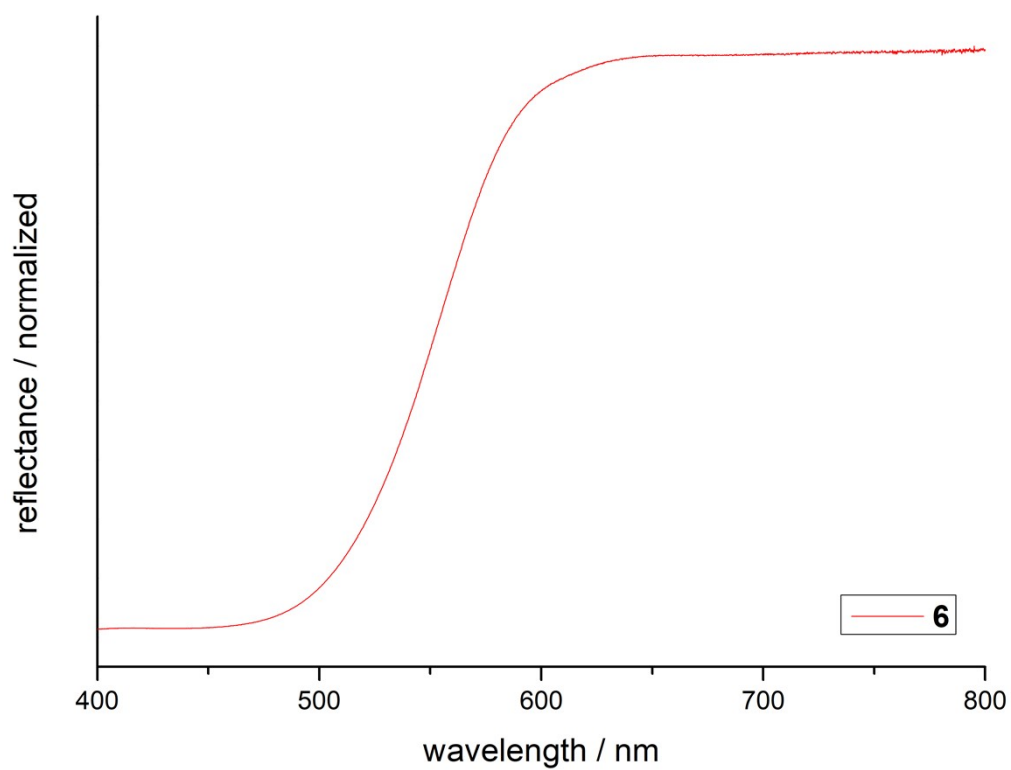


Figure S31. Raw UV-vis data of **6**.

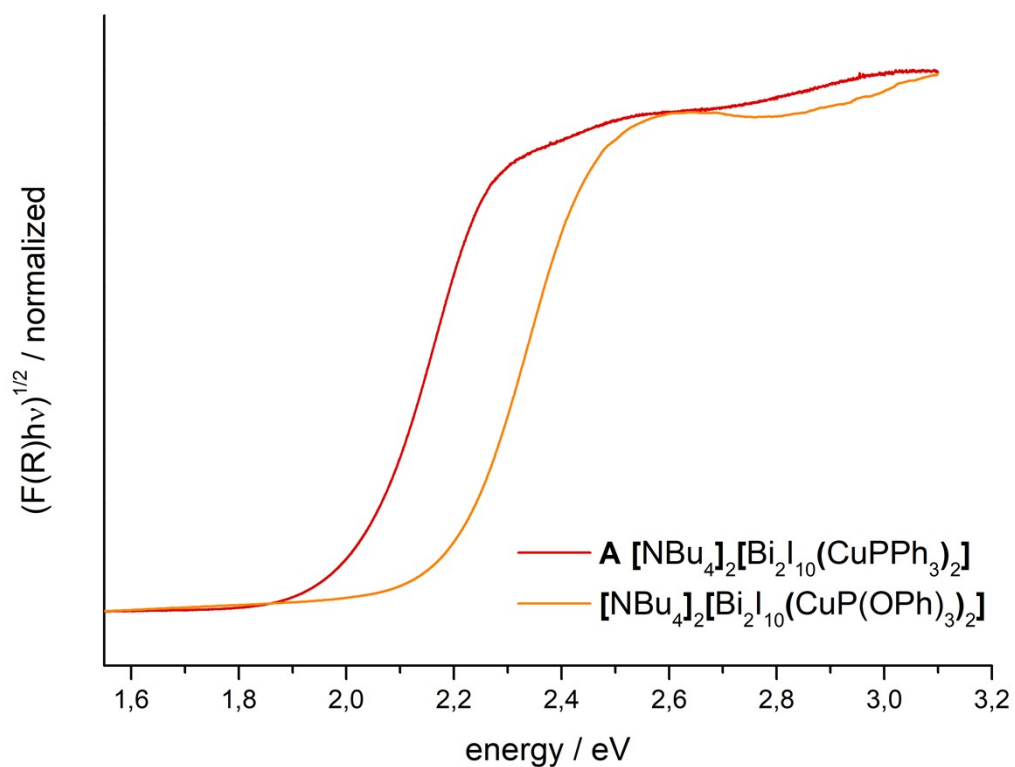


Figure S32. Tauc-plots from diffuse reflection UV-vis data of $[\text{NBu}_4]_2[\text{Bi}_2\text{I}_{10}(\text{CuPPh}_3)_2]$ (**A**) and $[\text{NBu}_4]_2[\text{Bi}_2\text{I}_{10}(\text{CuP(OPh)}_3)_2]$.

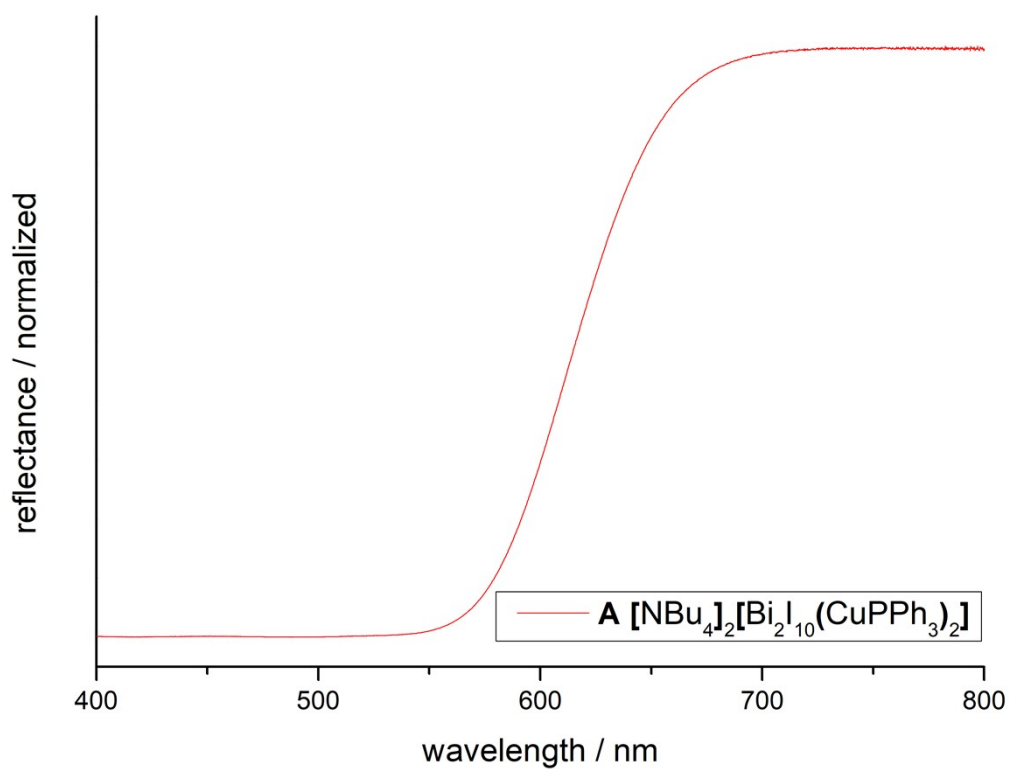


Figure S33. Raw UV-vis data of **A**.

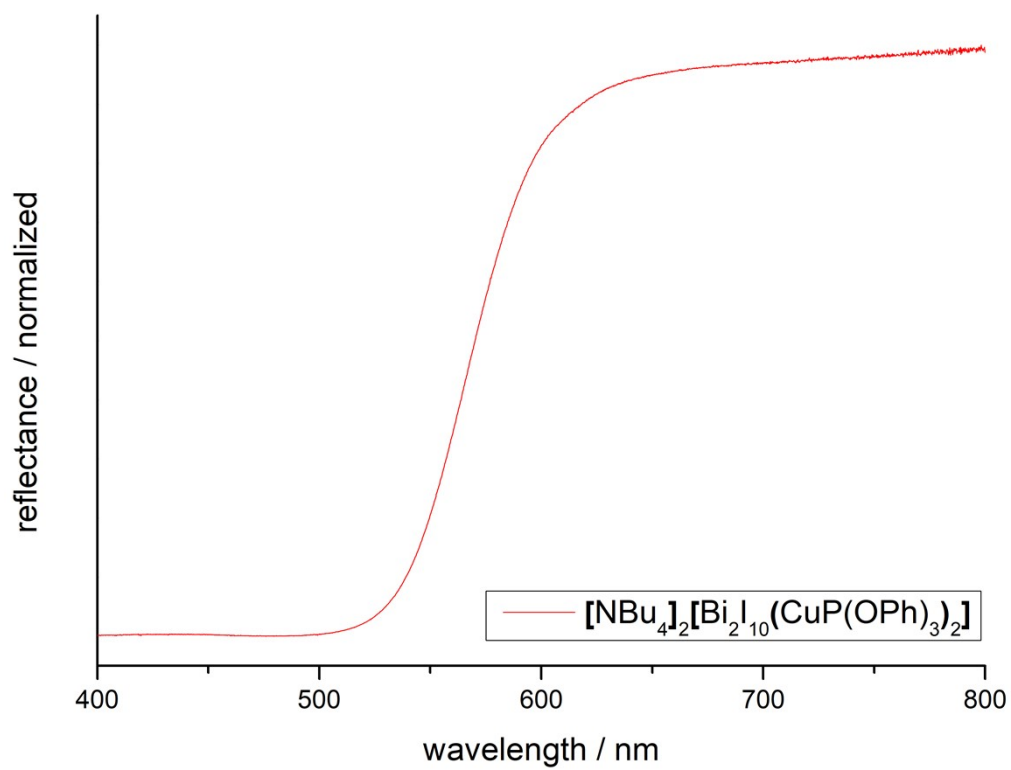


Figure S34. Raw UV-vis data of $[\text{NBu}_4]_2[\text{Bi}_2\text{I}_{10}(\text{CuP}(\text{OPh})_3)_2]$.

Powder diffraction

Powder patterns were recorded on a *STADI MP* (STOE Darmstadt) powder diffractometer, with $\text{CuK}_{\alpha 1}$ radiation with $\lambda = 1.54056 \text{ \AA}$ at room temperature in transmission mode. The patterns confirm the presence of the respective phase determined by SCXRD measurements and the absence of any major crystalline by-products unless otherwise indicated.

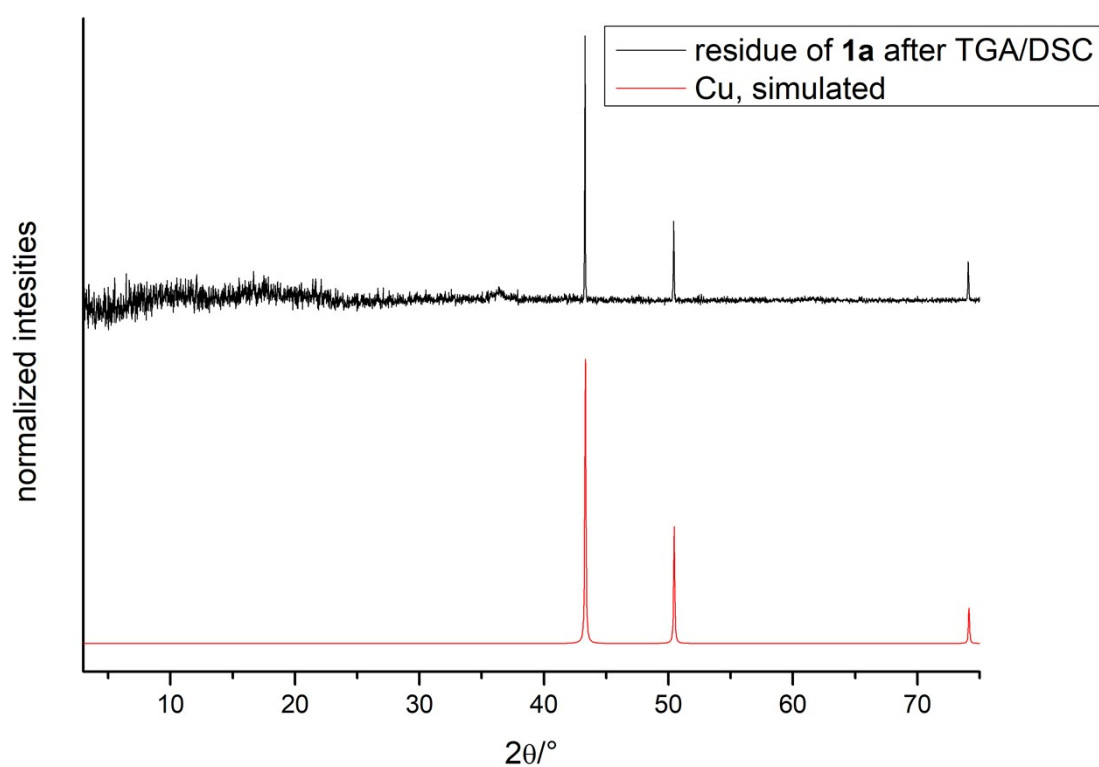


Figure S35: Powder diffraction pattern of the residue of **1a** after heating to 1000 °C under constant flow of N_2 -gas during TGA/DSC measurements. The reference pattern is simulated from literature data.⁵

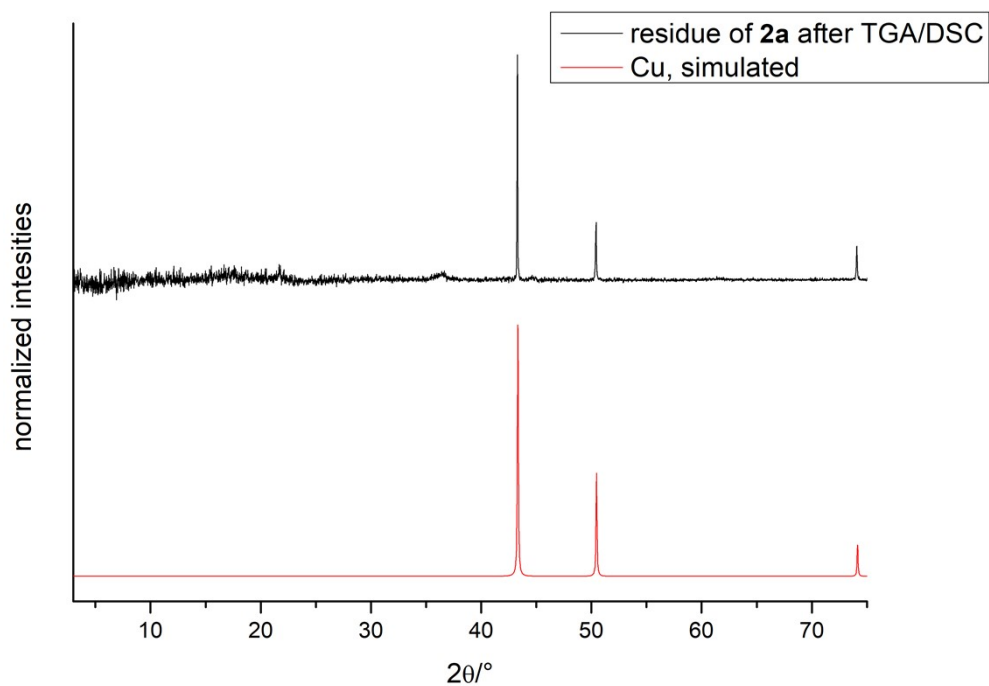


Figure S36: Powder diffraction pattern of the residue of **2a** after heating to 1000 °C under constant flow of N_2 -gas during TGA/DSC measurements. The reference pattern is simulated from literature data.⁵

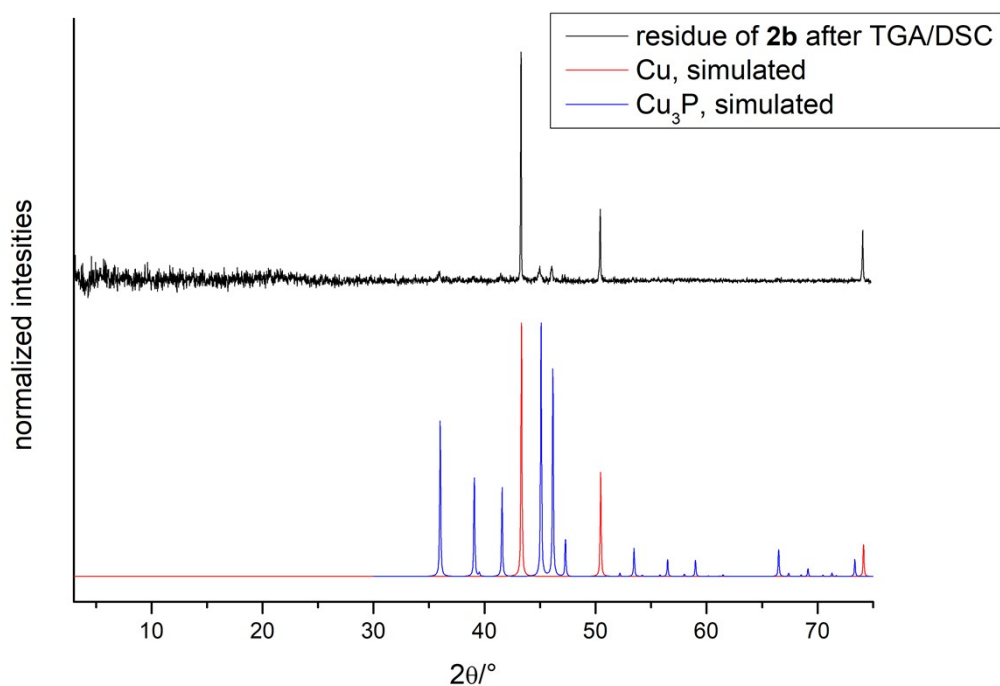


Figure S37: Powder diffraction pattern of the residue of **2b** after heating to 1000 °C under constant flow of N_2 -gas during TGA/DSC measurements. The reference pattern is simulated from literature data.^{5,6}

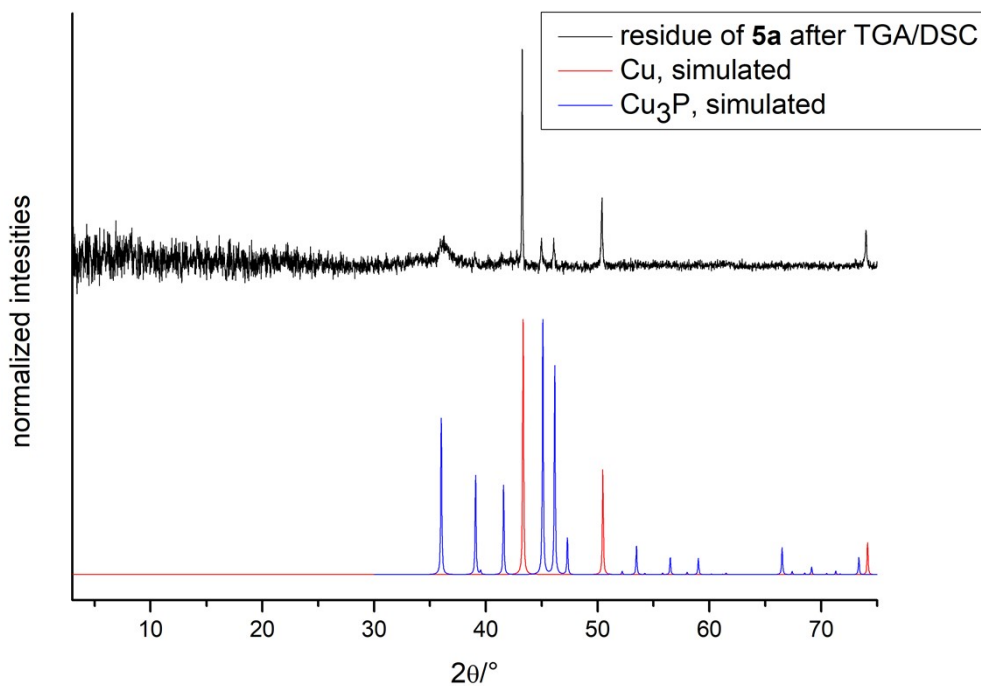


Figure S38: Powder diffraction pattern of the residue of **5a** after heating to 1000 °C under constant flow of N₂-gas during TGA/DSC measurements. The reference pattern is simulated from literature data.^{5,6}

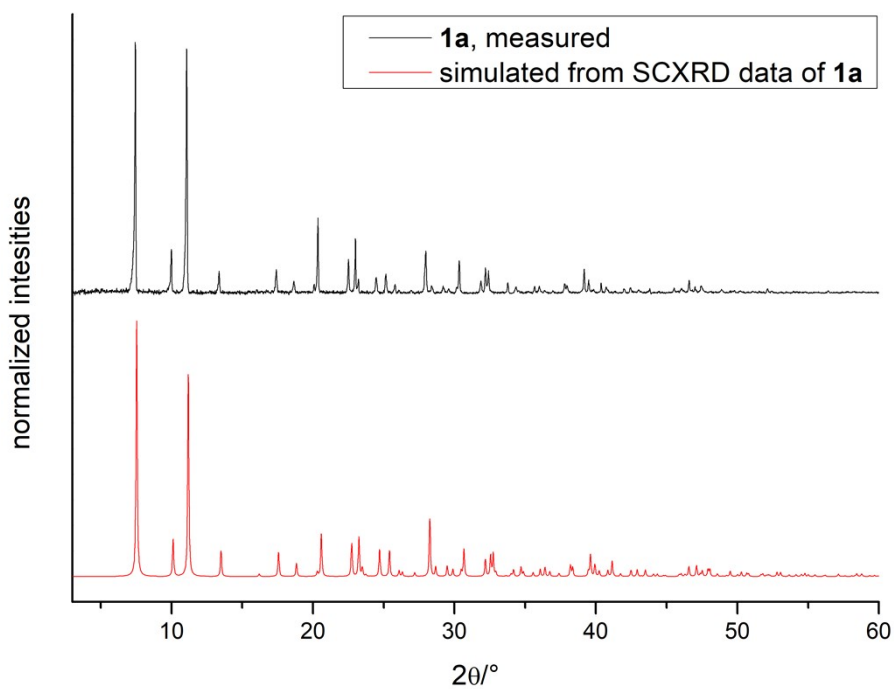


Figure S39. Powder diffraction pattern of **1a**.

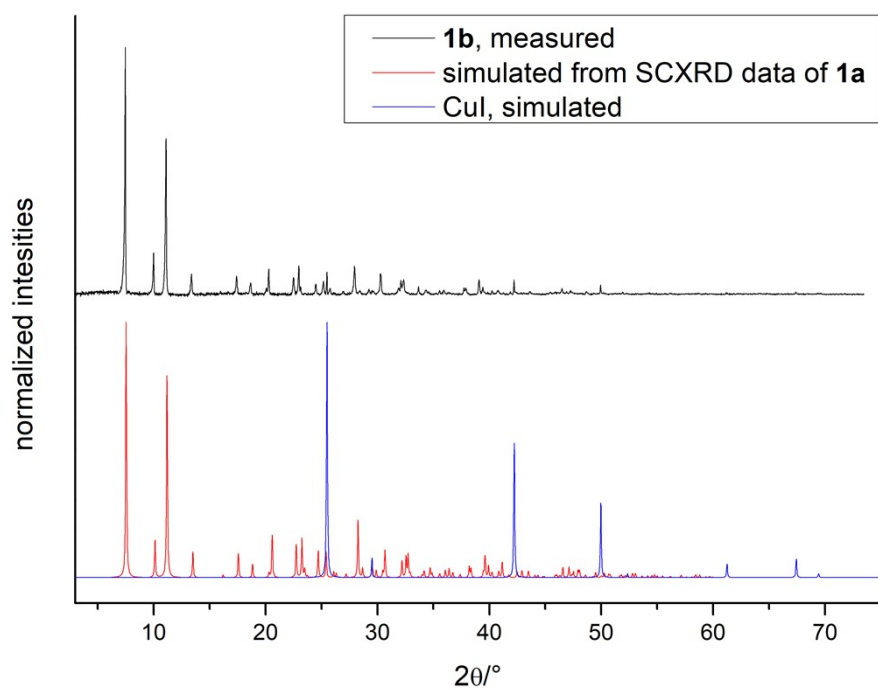


Figure S40. Powder diffraction pattern of **1b**. Since no single crystal data of **1b** could be obtained, data from the isostructural **1a** was chosen for comparison. The CuI reference pattern is simulated from literature data.⁷

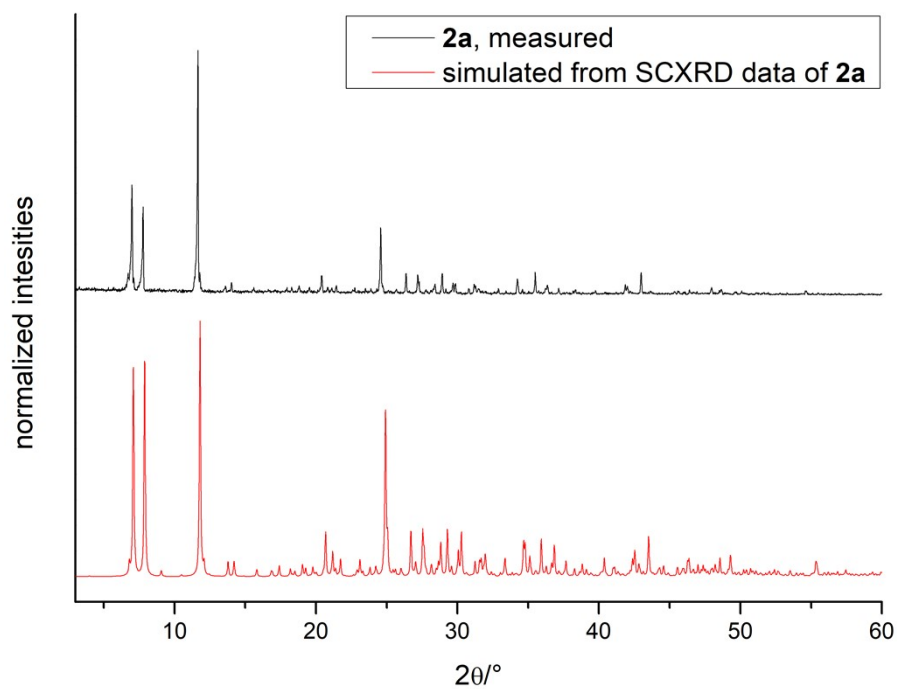


Figure S41. Powder diffraction pattern of **2a**.

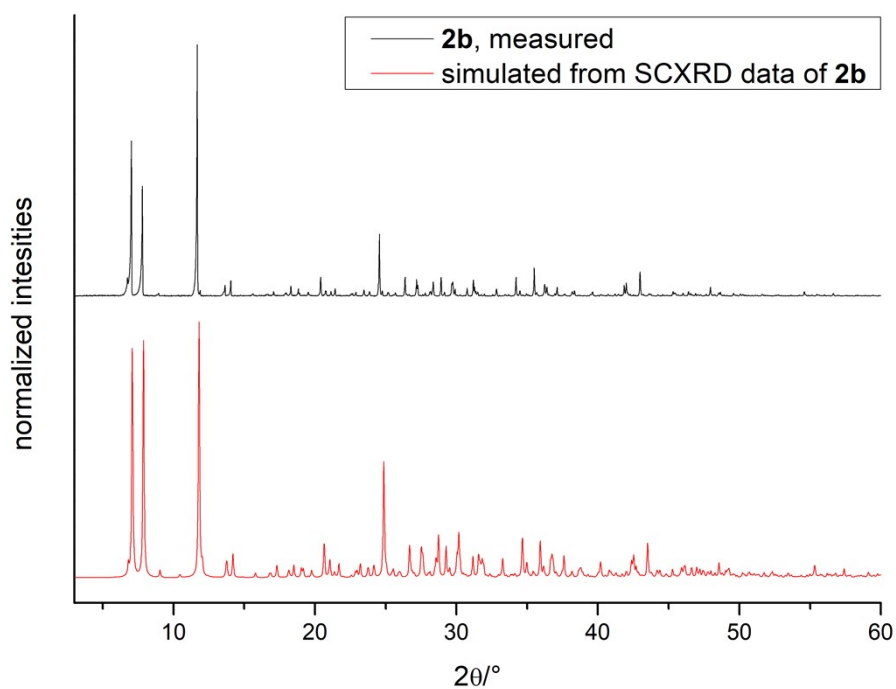


Figure S42. Powder diffraction pattern of **2b**.

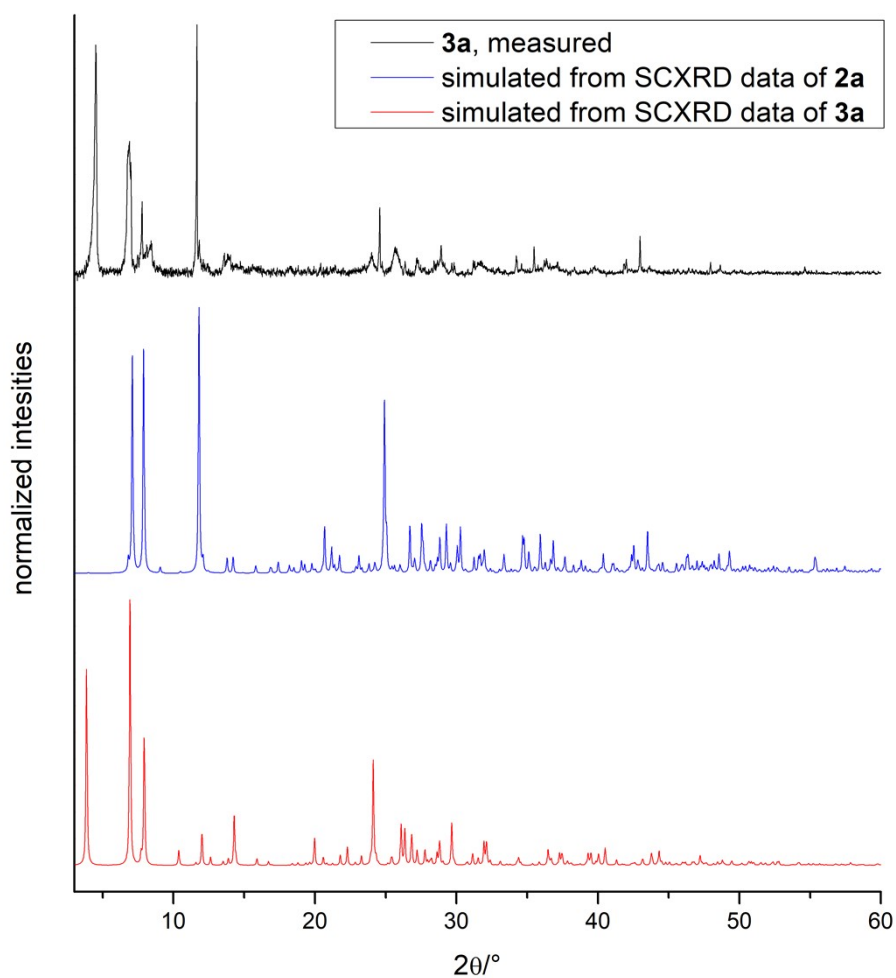


Figure S43. Powder diffraction pattern of **3a**. Comparison to simulated patterns of **3a** and the decomposition product **2a**.

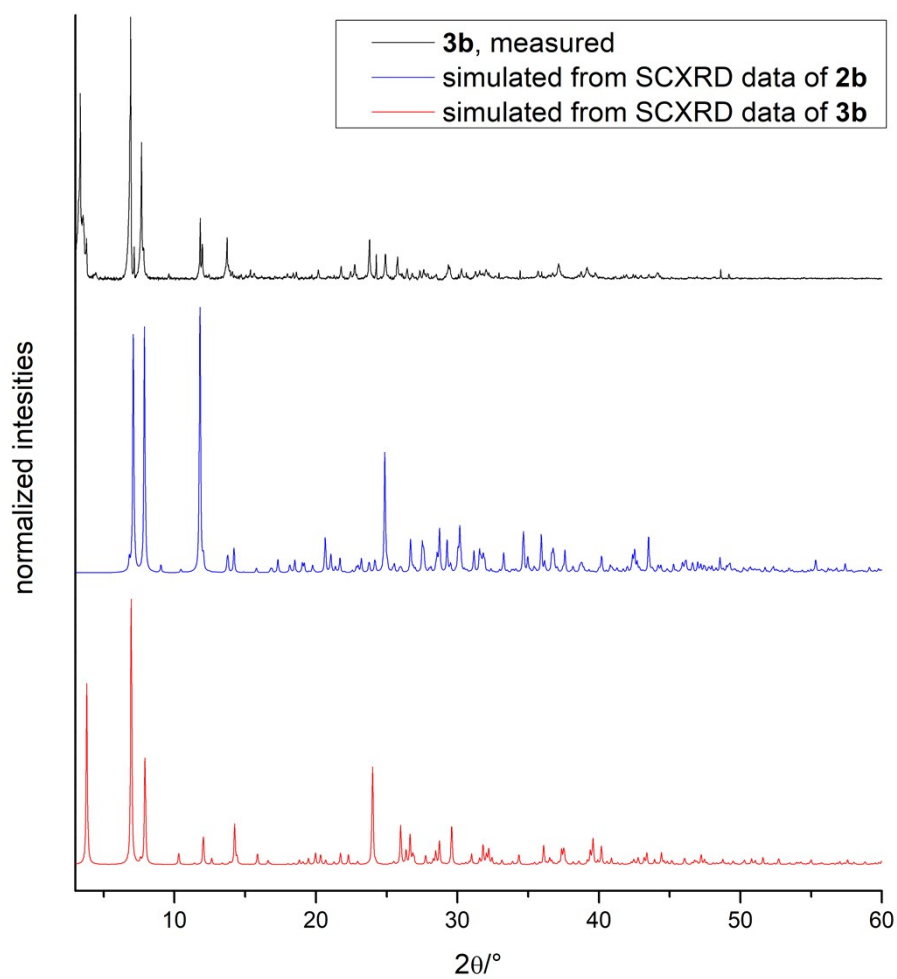


Figure S44. Powder diffraction pattern of **3b**. Comparison to simulated patterns of **3b** and the decomposition product **2b**.

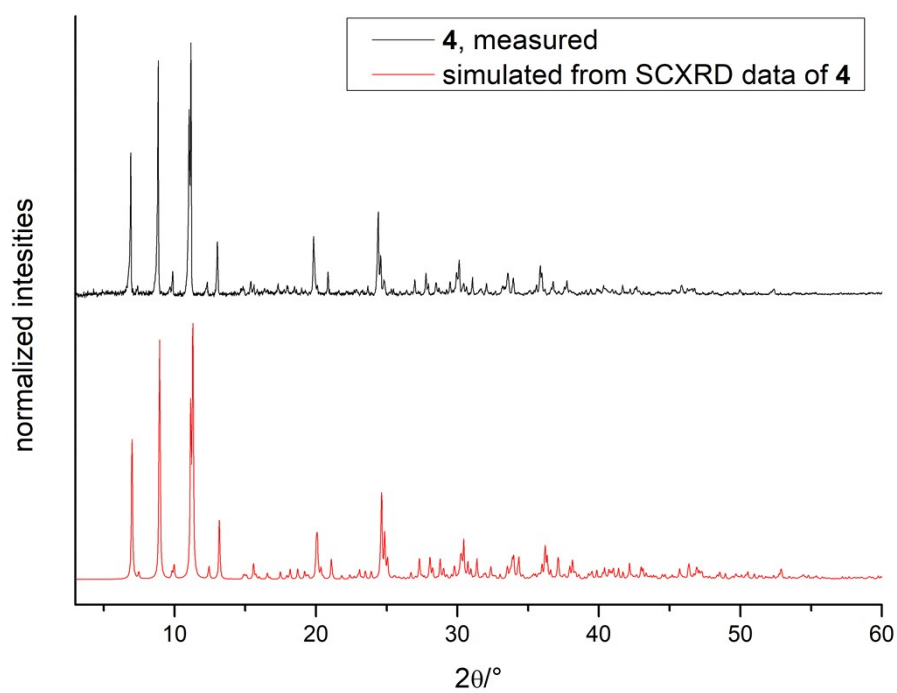


Figure S45. Powder diffraction pattern of **4**.

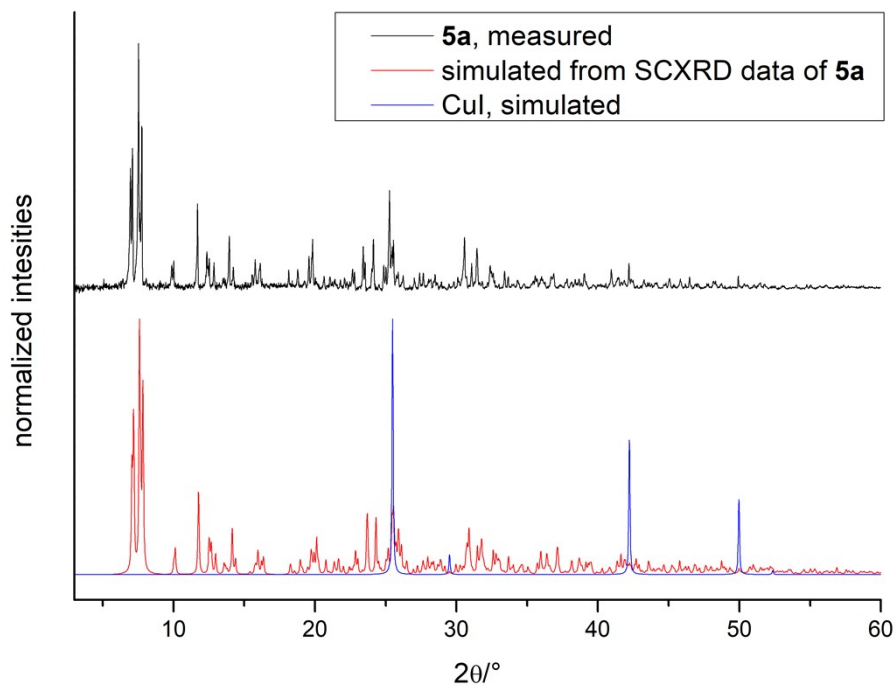


Figure S46. Powder diffraction pattern of **5a**. The CuI reference pattern is simulated from literature data.⁷

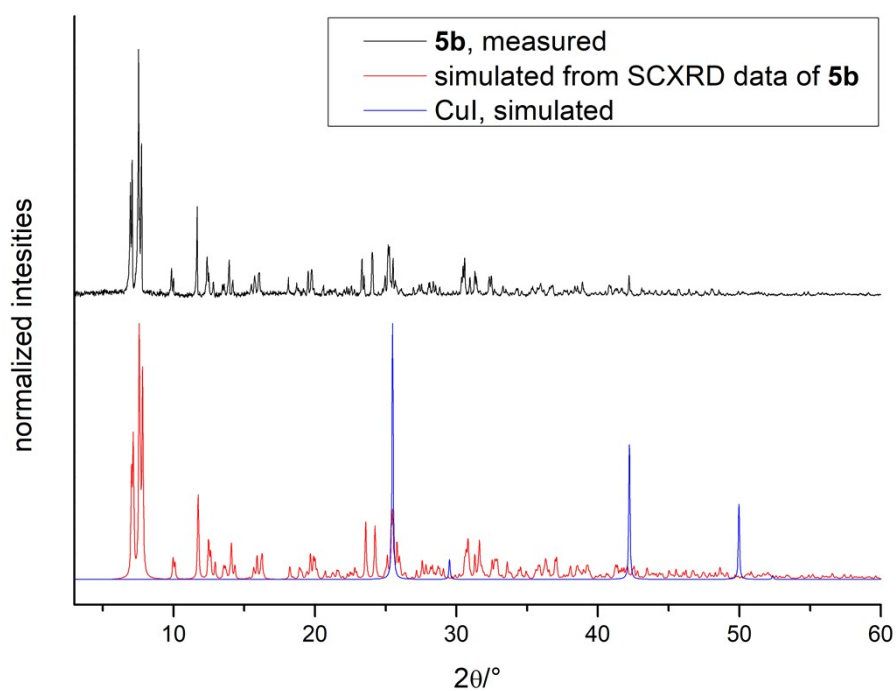


Figure S47. Powder diffraction pattern of **5a**. The CuI reference pattern is simulated from literature data.⁷

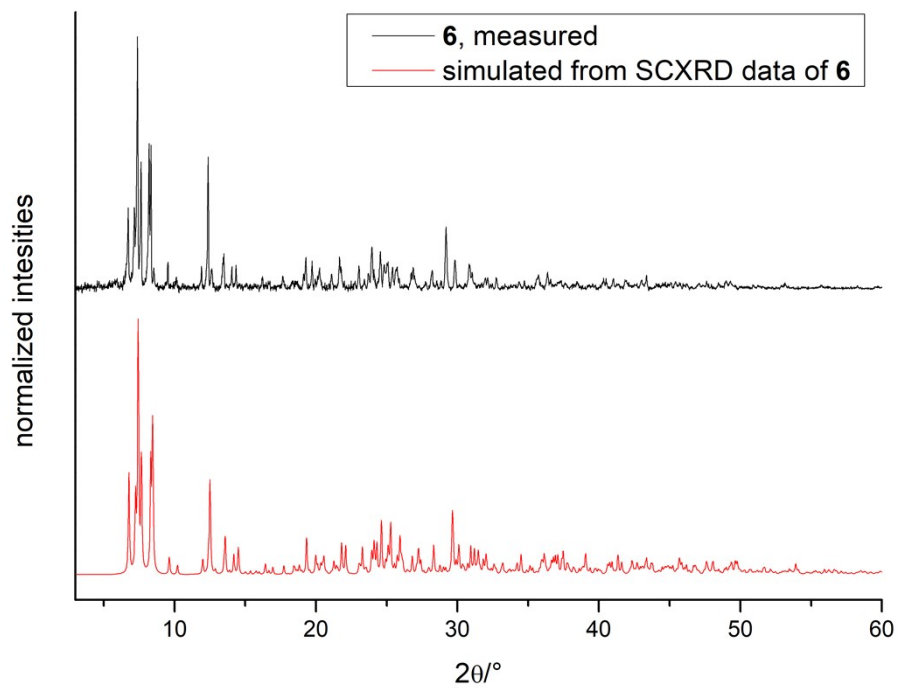


Figure S48. Powder diffraction pattern of **6**.

IR spectroscopy

IR spectra were recorded on a *Bruker Tensor 37* FT-IR spectrometer equipped with an ATR-Platinum measuring unit.

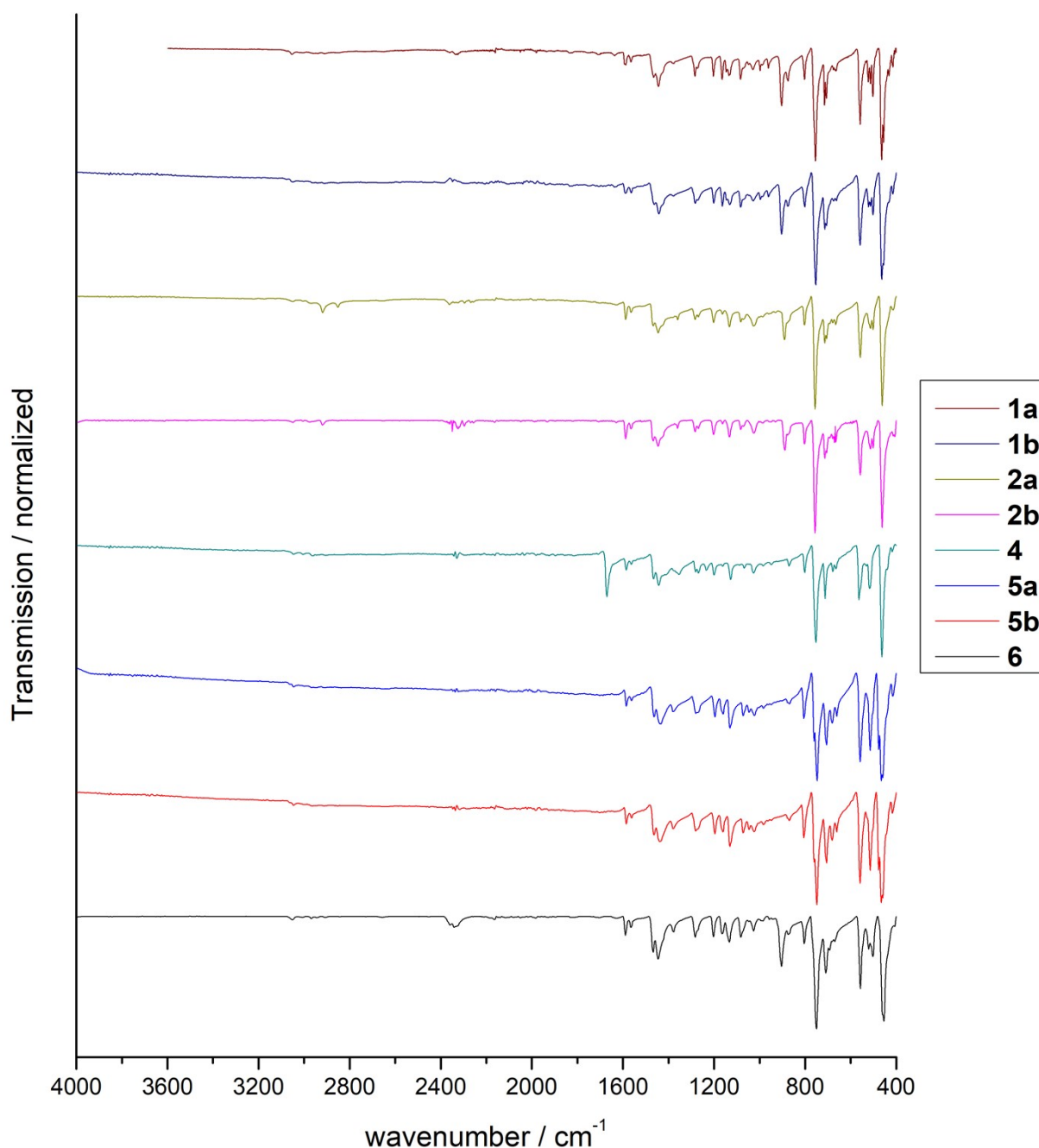


Figure S49. IR spectra of compound **1a**, **1b**, **2a**, **2b**, **4**, **5a**, **5b** and **6**. All spectra are very similar and dominated by bands of the tolyl groups in the 400 – 1800 cm^{-1} -region. The only exception is **4** where one strong additional band at 1671 cm^{-1} is observed. This can be assigned to the C=O valence vibration of the acetone ligand which is unique to **4**. The very weak bands between 2900 cm^{-1} and 3100 cm^{-1} can be assigned the C-H valence vibrations.⁸ The group of bands around 2300 cm^{-1} are an artefact of the atmospheric CO_2 compensation applied by the spectrometer software.

Theoretical investigations

Raw data is available at the NOMAD archive.

DOI: <https://dx.doi.org/10.17172/NOMAD/2021.08.06-1>

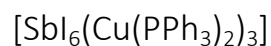


Table S15. First 15 spin-orbit states of $[\text{SbI}_6(\text{Cu}(\text{PPh}_3)_2)_3]$.

Spin-orbit state	$\Delta E_{\text{gap}} / \text{eV}$
1	1.9612
2	1.9644
3	1.9829
4	1.9899
5	1.9945
6	2.0069
7	2.0160
8	2.0398
9	2.0697
10	2.0742
11	2.0803
12	2.0830
13	2.2222
14	2.2228
15	2.2278

Table S16. Contributions of spin-free states to spin-orbit state 1 of $[\text{SbI}_6(\text{Cu}(\text{PPh}_3)_2)_3]$.

Spin-free state (%)	Molecular orbital contributions (%)	Character
T ₁ (45)	HOMO→LUMO (100)	Cu-d→Sb-p
T ₄ (25)	HOMO→LUMO+1 (98)	Cu-d→Sb-p
T ₇ (8)	HOMO-3→LUMO (88)	Sb-s→Sb-p
T ₁₁ (7)	HOMO→LUMO+2 (98)	Cu-d→Sb-p

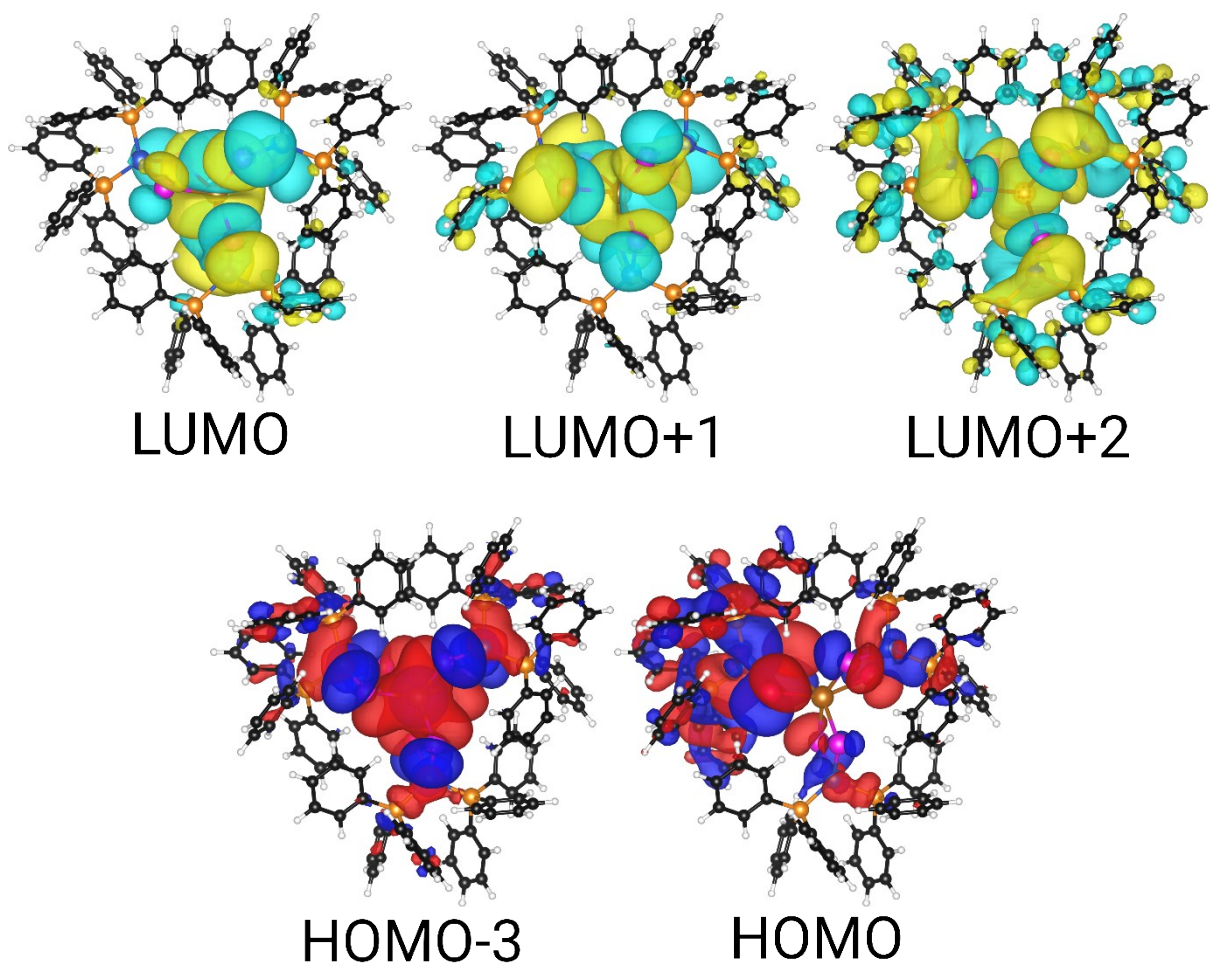


Figure S50. Relevant molecular orbitals of $[\text{SbI}_6(\text{Cu}(\text{PPh}_3)_2)_3]$.

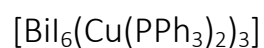
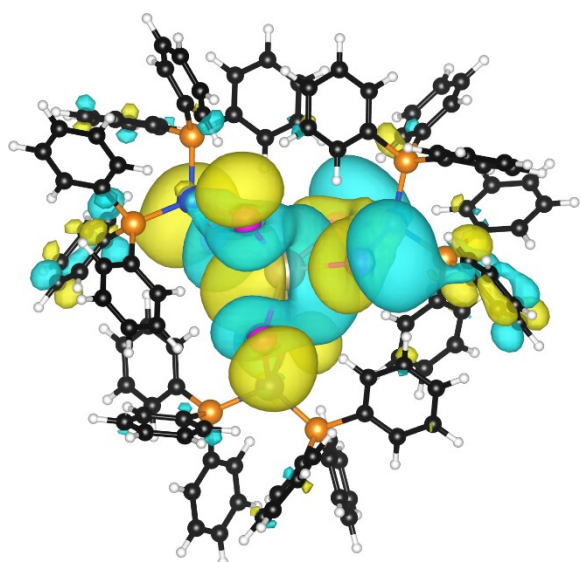


Table S17. First 15 spin-orbit states of [Bi₆(Cu(PPh₃)₂)₃].

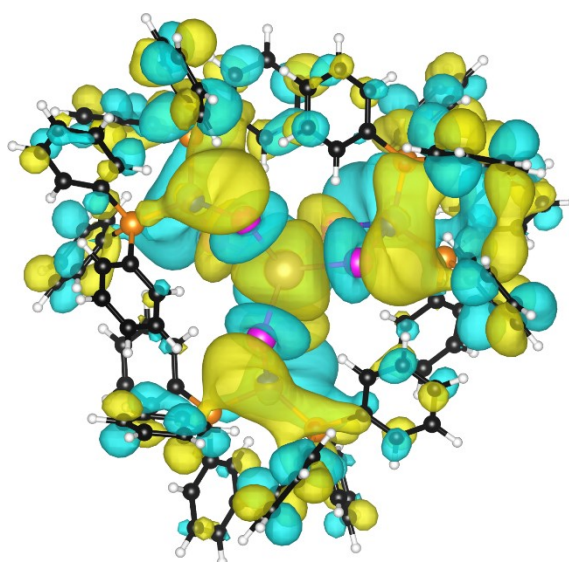
Spin-orbit state	$\Delta E_{\text{gap}} / \text{eV}$
1	1.3387
2	1.3451
3	1.3534
4	1.3768
5	1.3804
6	1.3868
7	1.3945
8	1.4127
9	1.4796
10	1.4859
11	1.4928
12	1.4943
13	1.9625
14	1.9776
15	2.0033

Table S18. Contributions of spin-free states to spin-orbit state 1 of [Bi₆(Cu(PPh₃)₂)₃].

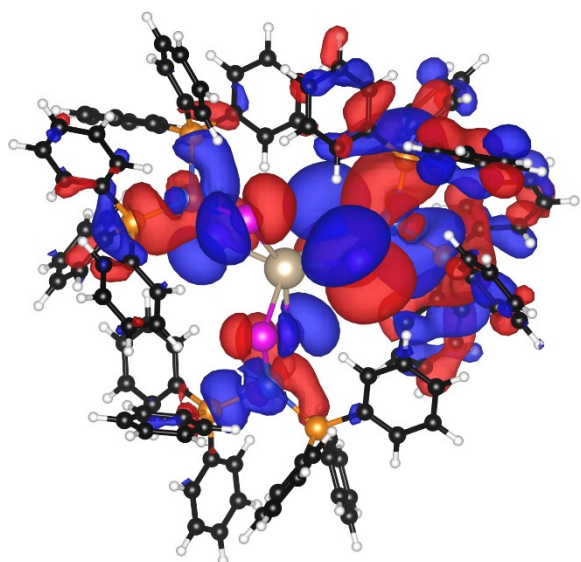
Spin-free state (%)	Molecular orbital contributions (%)	Character
T ₁ (29)	HOMO→LUMO (100)	Cu-d→Bi-p
T ₄ (27)	HOMO→LUMO+1 (99)	Cu-d→Bi-p
S ₉ (8)	HOMO→LUMO+2 (97)	Cu-d→Bi-p



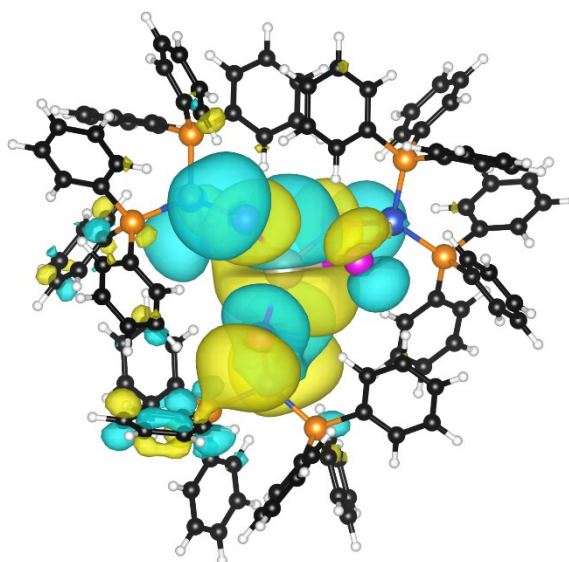
LUMO+1



LUMO+2



HOMO



LUMO

Figure S51. Relevant molecular orbitals of $[\text{Bi}_6(\text{Cu}(\text{PPh}_3)_2)_3]$.

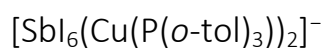


Table S19. First 15 spin-orbit states of $[\text{SbI}_6(\text{Cu}(\text{P}(\text{o-tol})_3)_2)]^-$.

Spin-orbit state	$\Delta E_{\text{gap}} / \text{eV}$
1	2.3849
2	2.4052
3	2.4066
4	2.4332
5	2.4391
6	2.4465
7	2.4570
8	2.4649
9	2.5092
10	2.5200
11	2.5214
12	2.5227
13	2.5240
14	2.5261
15	2.5264

Table S20. Contributions of spin-free states to spin-orbit state 1 of $[\text{SbI}_6(\text{Cu}(\text{P}(\text{o-tol})_3)_2)]^-$.

Spin-free state (%)	Molecular orbital contributions (%)	Character
T ₇ (19)	HOMO→LUMO+4 (92)	Cu-d→Sb-p
T ₁ (17)	HOMO→LUMO (97)	Cu-d→π*
T ₁₀ (17)	HOMO→LUMO+5 (77)	Cu-d→Sb-p
T ₁₉ (15)	HOMO→LUMO+6 (97)	Cu-d→Sb-p
T ₂ (14)	HOMO→LUMO+1 (91)	Cu-d→π*
T ₂₀ (5)	HOMO-3→LUMO (65)	Cu-d→π*

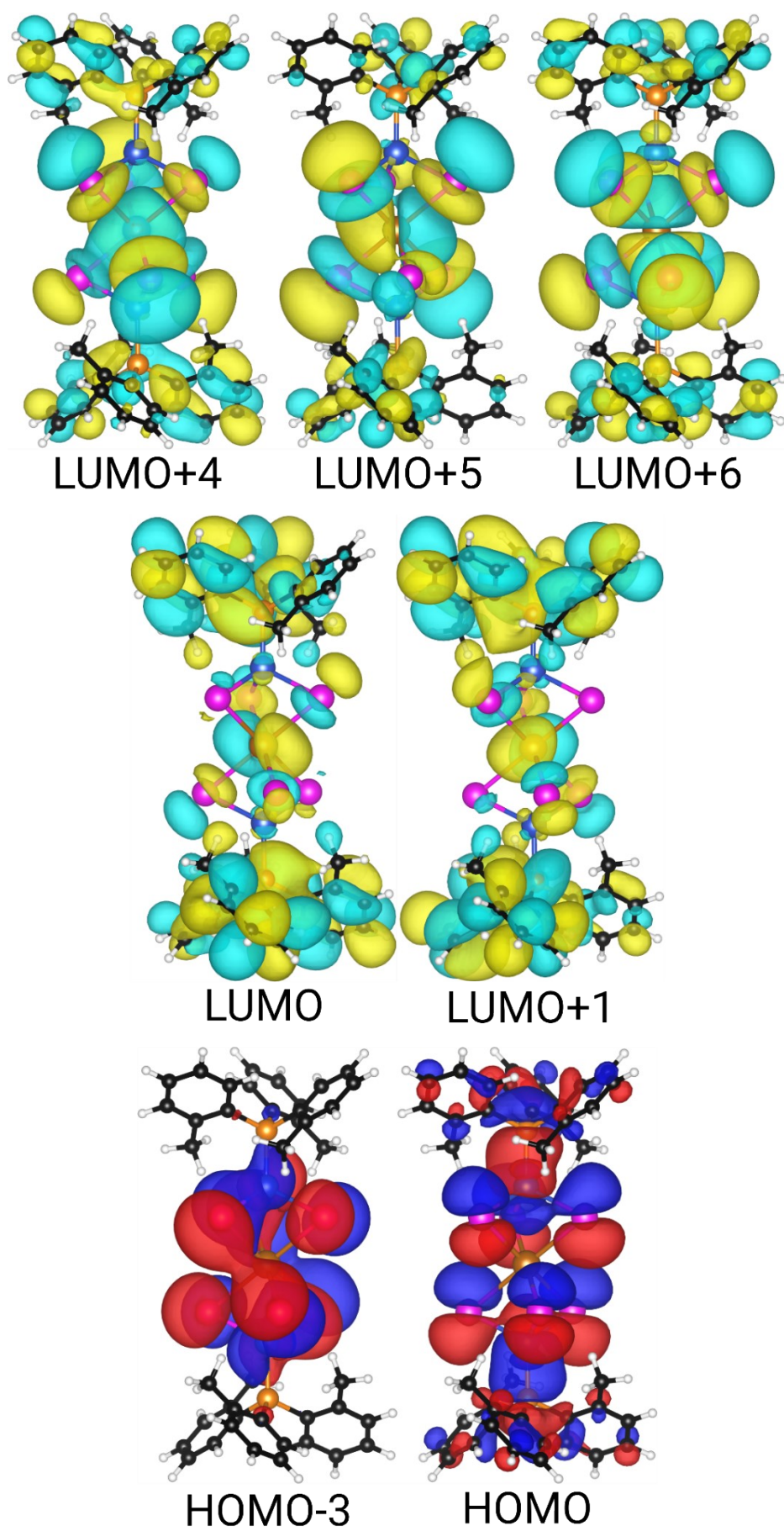
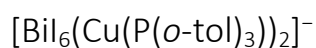
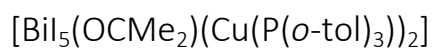


Figure S52. Relevant molecular orbitals of $[\text{SbI}_6(\text{Cu}(\text{P}(\text{o-tol})_3)_2)]^-$.

**Table S21.** First 15 spin-orbit states of $[\text{Bi}_6(\text{Cu}(\text{P}(\text{o-tol})_3)_2)]^-$.

Spin-orbit state	$\Delta E_{\text{gap}} / \text{eV}$
1	2.0252
2	2.0254
3	2.1048
4	2.1088
5	2.2416
6	2.2419
7	2.4946
8	2.5083
9	2.5113
10	2.5157
11	2.5272
12	2.5286
13	2.5312
14	2.5384
15	2.5397

**Table S22.** First 15 spin-orbit states of $[\text{Bi}_5(\text{OCMe}_2)(\text{Cu}(\text{P}(\text{o-tol})_3)_2)]$.

Spin-orbit state	$\Delta E_{\text{gap}} / \text{eV}$
1	1.6566
2	1.6966
3	1.7184
4	1.8441
5	2.0598
6	2.0771
7	2.1173
8	2.1619
9	2.2331
10	2.2406
11	2.2662
12	2.3082
13	2.5396
14	2.5475
15	2.5488

Table S23. Contributions of spin-free states to spin-orbit state 1 of $[\text{Bi}_5(\text{OCMe}_2)(\text{Cu}(\text{P}(o\text{-tol})_3))_2]$.

Spin-free state (%)	Molecular orbital contributions (%)	Character
T ₄ (34)	HOMO→LUMO+1 (99)	Cu-d→Bi-p+OCMe
T ₁₆ (22)	HOMO→LUMO+4 (91)	Cu-d→Bi-p+π*
T ₁₂ (21)	HOMO→LUMO+3 (97)	Cu-d→Bi-p+OCMe
T ₁ (11)	HOMO→LUMO (100)	Cu-d→Bi-p+OCMe

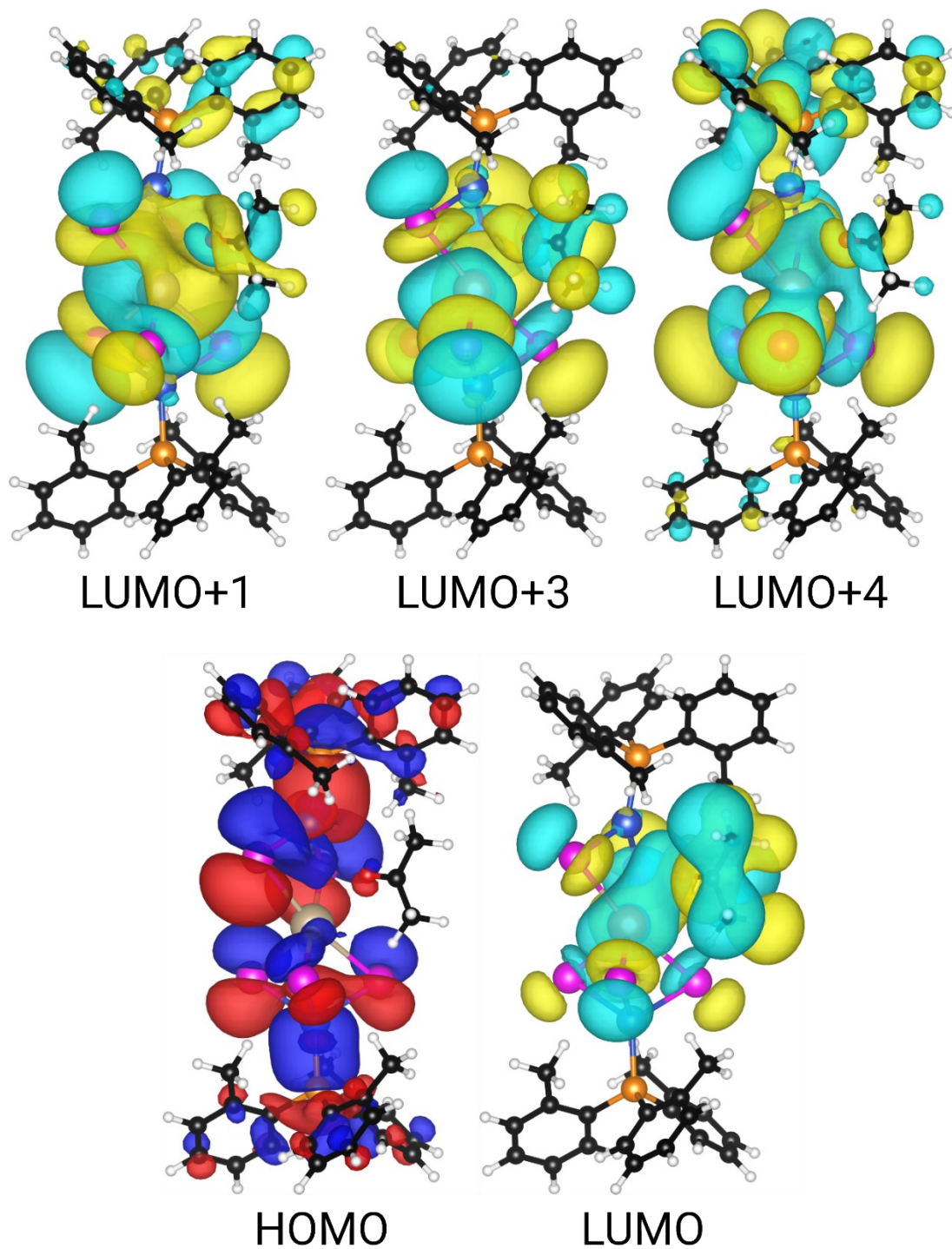


Figure S53. Relevant molecular orbitals of $[\text{Bi}_5(\text{OCMe}_2)(\text{Cu}(\text{P}(o\text{-tol})_3))_2]$.

References

- [1] A. W. Kelly, A. M. Wheaton, A. D. Nicholas, F. H. Barnes, H. H. Patterson, R. D. Pike, *Eur. J. Inorg. Chem.* 2017, 4990.
- [2] D. Kratzert, J. J. Holstein and I. Krossing, *J. Appl. Crystallogr.*, 2015, **48**, 933.
- [3] K. A. Michalow, D. Logvinovich, A. Weidenkaff, M. Amberg, G. Fortunato, A. Heel, T. Graule and M. Rekas, *Catalysis Today*, 2009, **144**, 7.
- [4] P. Makuła, M. Pacia and W. Macyk, *J. Phys. Chem. Lett.*, 2018, **9**, 6814.
- [5] H. Kasai, L. Song, H. L. Andersen, H. Yin and B. B. Iversen, *Acta Crystallogr., Sect. B: Struct. Sci., Cryst. Eng. Mater.*, 2017, **73**, 1158.
- [6] R. O. Demchyna, S. I. Chykhrij and Y. B. Kuz'ma, *J. Alloys Compd.*, 2002, **345**, 170.
- [7] M. Yashima, Q. Xu, A. Yoshiasa and S. Wada, *J. Mater. Chem.*, 2006, **16**, 4393.
- [8] H. G. O. Becker, *Organikum. Organisch-chemisches Grundpraktikum*, Wiley-VCH, Weinheim, 21st ed., 2001.